GLASS FIBER REINFORCED EPOXY NANOCOMPOSITES: INFLUENCE OF POSTCURING AND NANOCLAY CONTENT ON MECHANICAL PROPERTIES

A

Thesis Report

Submitted in partial fulfilment of the requirement for the award of degree

MASTER OF ENGINEERING
in
CAD/CAM & ROBOTICS

Submitted By
Mahakdeep Singh
(Roll No. 801081017)

Under Guidance of

Mr. BIKRAMJIT SHARMA
Assistant Professor
Deptt. Of Mechanical Engg.
Thapar University, Patiala

Dr. RAJEEV MEHTA
H.O.D & Associate Professor
Deptt. Of Chemical Engg.
Thapar University, Patiala

MECHANICAL ENGINEERING DEPARTMENT

THAPAR UNIVERSITY, PATIALA-147004, INDIA

July 2012

CERTIFICATE

This is to certify that the work in this thesis report entitled "**Glass Fiber Reinforced Epoxy Nanocomposites: Influence of Postcuring and Nanoclay content on Mechanical properties**" submitted in partial fulfilment of requirement for the award of **Master Of Engineering Degree in CAD/CAM & Robotics** in Mechanical Department of Thapar University, Patiala, is an authentic record of work carried out by me under the guidance of **Mr. Bikramjit Sharma**, Assistant Professor, Mechanical Engineering Department, Thapar University, Patiala and **Dr. Rajeev Mehta**, H.O.D & Associate Professor, Chemical Engineering Department, Thapar University, Patiala.

The matter embodied in this report has not been submitted in part or full to any university or institute for the award of any degree.

Mahakdeep Singh

Dated: 15.07.2012 **Mahakdeep Singh**

This is to certify that the above declaration made by the student concern is correct to the best of my knowledge and belief.

Mr. Bikramjit Sharma
Assistant Professor
Deptt. Of Mechanical Engg.
Thapar University, Patiala.

Dr. Rajeev Mehta
H.O.D & Associate Prof.
Deptt. Of Chemical Engg.
Thapar University, Patiala.

Countersigned By:

Dr. Ajay Batish
Professor & Head M.E.D
Thapar University, Patiala.

Dr. S. K. Mohapatra
Dean Academics Affairs
Thapar University, Patiala.

ACKNOWLEDGEMENT

I am highly grateful to the authorities of Thapar University, Patiala for providing this opportunity to carry out the Thesis work.

I would like to express a deep sense of gratitude and thank profusely my thesis guide **Mr. Bikramjit Sharma**, Assistant Professor, Mechanical Engineering Department, Thapar University, Patiala and **Dr. Rajeev Mehta**, H.O.D. & Associate Professor, Chemical Engineering Department, Thapar University, Patiala for their sincere & invaluable guidance, suggestions and attitude which inspired me to submit report in the present form.

I am highly thankful to **Mr. Toyesh** (Ph.D Scholar in Chemical Engineering Department) for his invaluable guidance & continuous support.

I am also thankful to other faculty members and all the workshop staff of Mechanical Department, Thapar University, Patiala for their support.

I would also like to thank and acknowledge **BASF Construction Chemicals (India) Private Limited and Connell Bros. Mumbai** for supplying us generously with E-Glass Fibre sheet, M Brace epoxy (Base and hardener) and Clay (Closite 30B) etc. for this experimentation.

My special thanks are due to my family members and friends who constantly encouraged me to complete this study.

Mahakdeep Singh

MAHAKDEEP SINGH

ABSTRACT

Nanocomposites are as a multiphase solid material where one of the phases has one, two or three dimensions of less than 100 nanometer (nm). These differ from conventional composites due to the exceptionally high surface to volume ratio of the reinforcing phase and/or its exceptionally high aspect ratio. In the present work epoxy modified with Closite 30B® nanoclay added at different concentrations (0.5wt%, 2wt%, 3wt% and 4wt %) is used as matrix with unidirectional glass fibers to manufacture laminates having [0^0, 90^0 ,0^0] stacking sequence . The samples were then cured under different conditions (I) Normal temperature and ambient conditions for 12 hrs (II) At 100^0C in Vaccum oven for 4 hours (III) A combination of I &II. X-Ray Diffraction of Epoxy/Clay nanocomposites indicates exfoliation of nanoclay at all loadings .The mechanical tests shows an increase in the tensile strength, flexural strength and micro hardness of nanocomposites with addition of nanoclay at small quantities. Significant improvement in properties was seen in all specimens as an effect of post curing at high temperatures. Further durability studies on nanocomposites have been performed in water and NaOH baths under accelerated hygrothermal loading. During exposure it is observed that the properties degradation in NaOH environment was more severe as compared to simple water. Results show that with postcuring of the samples under condition (III), the degradation of the specimen significantly reduced in comparison to samples cured under conditions I or II. This is probably due to more efficient crosslinking of the polymer .

TABLE OF CONTENT

LIST OF FIGURES

LIST OF TABLES

NOMENCLATURE AND ABBREVATIONS

GFRP	glass fiber reinforced polymer
VLSI	very large scale integration
PNC	polymer nanocomposites
POSS	Polyoctahedral silsesquioxane
OMMT	monomorillonite organoclay
CNF's	carbon nanofibers
CNT's	carbon nanotubes
XRD	X-Ray Diffraction
WXRD	wide angle x-ray diffraction
PAN	polyacrylonitrile
SEM	scanning electron microscope
CTE	coefficient of thermal expansion
VGCF	vapor grown carbon fiber
CAI	compression after impact

CHAPTER 1 INTRODUCTION

1.1 Nanocomposites

A nano-composite is as a multiphase solid material where one of the phases has one, two or three dimensions of less than 100 nanometer (nm), or structures having nano-scale repeat distances between the different phases that make up the material. In the broadest sense this definition can include porous media, colloids, gels and copolymer, but is more usually taken to mean the solid combination of a bulk matrix and nano-dimensional phase(s) differing in properties due to dissimilarities in structure and chemistry. The mechanical, electrical, thermal, optical, electrochemical, catalytic properties of the nano-composite will differ markedly from that of the component materials. Size limits for these effects have been proposed, <5 nm for catalytic activity, <20 nm for making a hard magnetic material soft, <50 nm for refractive index changes, and <100 nm for achieving superparamagnetism, mechanical strengthening or restricting matrix dislocation movement.

Nanocomposites are found in nature, for example in the structure of the abalone shell and bone. The use of nanoparticle-rich materials long predates the understanding of the physical and chemical nature of these materials. From the mid 1950s nanoscale organo-nanoclays have been used to control flow of polymer solutions (e.g. as paint viscosifiers) or the constitution of gels (e.g. as a thickening substance in cosmetics, keeping the preparations in homogeneous form). By the 1970s polymer/nano composites were the topic of textbooks, although the term "nanocomposites" was not in common use.

In mechanical terms, nanocomposites differ from conventional composites due to the exceptionally high surface to volume ratio of the reinforcing phase and/or its exceptionally high aspect ratio. The reinforcing material can be made up of particles (e.g. minerals), sheets (e.g. exfoliated nanoclay stacks) or fibers (e.g. carbon nanotubes or electrospun fibers). The area of the interface between the matrix and reinforcement phase(s) is typically an order of magnitude greater than for conventional composite materials. The matrix material properties are significantly affected in the vicinity of the reinforcement. Ajayan *et al.* (1992) observed that with polymer nanocomposites, properties related to local chemistry, degree of thermoset cure, polymer chain mobility, polymer chain conformation, degree of polymer chain ordering or

crystallinity can all vary significantly and continuously from the interface with the reinforcement into the bulk of the matrix.

Advantages of nanocomposites:

• Greater tensile and flexural strength for the same dimension of plastic part
• Reduced weight for the same performance
• Improved mechanical strength
• Improved gas barrier properties for the same film thickness
• Higher chemical resistance

1.2 Polymer nanocomposites

Polymer layered nanocomposites have been investigated by academic and industrial researches in recent years because the final composites often provide a desired enhancement of mechanical, molecular barrier, thermal, flame retardant, corrosion protection properties and/or other properties relative to the original polymer matrix, even at very low nanoclay contents . Nanoparticles may dominate the behavior of materials because of their sizes, nanoscale dimensions, and relatively huge surface areas per unit weight. Carbon nanotubes, montmorillonite type nanoclays and bimolecules such as protein and DNA are used in many nanostructures . Polymeric properties can be improved even at low loading without negative effects on density, transparency and processability. Basically, nanoparticles are dispersed in a polymer matrix at low amounts, most of the time less than 6% by weight . The conditions for successful reinforcement and good properties are the homogeneous distribution and dispersion of the reinforcing components, high aspect ratio of the nanolevel fillers, and good adhesion between polymer matrix and fillers . Many thermoplastic and thermosetting polymers with different polarities including polystyrene, polycaprolactone, polypropylene, poly(ethylene oxide), epoxy resin, polysiloxane and polyurethane can be used to form nanocomposite structures. The first commercial product of nanoclay-based polymer nanocomposites was the timing belt cover made from PA6 nanocomposites by Toyota Motors in the early 1990s A nanocomposite can be defined as a particle-filled polymer which has at least one dimension of dispersed particles in the nanometer range . We can classify the nanocomposites according to the dimension ranges of the dispersed particles. When we mention the three dimensions which are all in the order of nanometers, we are talking about isodimensional nanoparticles, such as spherical silica

nanoparticles, semiconductor nanoclusters, and others . Carbon nanotubes or cellulose whiskers can be classified separately in which two dimensions are in nanometer scale, and the third one is larger while forming an elongated structure . In the last group, one dimensional fillers exist which are typically a few nanometers thick and a few thousand nanometers long. Polymer-layered crystal or nanoclay nanocomposite is the general name of this group . Nanocomposites cannot be formed only by physical mixing of the polymer and inorganic materials. The problem is the polymer blends; most of the time immiscible systems cause poor mechanical attraction and particle agglomeration between the polymer and inorganic materials. Therefore, phase separated composite, which is similar to the traditional microcomposites, is obtained when the polymer is not capable to intercalate between silicate sheets .

1.3 Morphology of nanocomposites

When layered silicates organically modified and dispersed within a polymer, the spacing expands to allow for the intercalation of polymer between the unit layers. Depending on the nature of the layered nanoclay and polymer matrix and the level of interactions between them, three different types of polymer nanocomposite morphology are observed. These are: intercalated, exfoliated and phase separated.

1. Phase separated composites: Layered silicates exist in their original aggregated state with no intercalation of the polymer matrix into the galleries (Figure 1.1). In this case, the particles act as microscale fillers. Their properties stay in the same range as seen in traditional microcomposites.

2. Intercalated composites: When polymer resin is inserted into the gallery between the adjacent layers, the spacing expands, and it is known as the intercalated state (Figure 1.1). In the intercalated form, matrix polymer molecules are introduced between the ordered layers of silicate resulting in an increase in the interlayer spacing, but still maintaining the order.

3. Exfoliated composites: In exfoliated nanocomposites, the individual nm scale thick silicate layers are separated and dispersed in a continuous polymer matrix with average distances between layers depending on the silicate concentration (Figure 1.1). When the layers are fully separated, the silicate is considered to be exfoliated. Exfoliated nanocomposites improve specific properties better than intercalated one, that are affected by the degree of dispersion and resulting interfacial area between polymer and silicate nanolayers.

In addition, **Partially Intercalated or Exfoliated Composite** morphology may also be obtained. In this commonly occurring case, the exfoliated layers and intercalated clusters are randomly

distributed in the matrix. The final structure of silicate composite has a wide range of variations, depending on the degree of intercalation and exfoliation. X-ray diffraction measurements are used to characterize the intercalation and exfoliation structures. Reflections in the low angle region indicate intercalated composite, but if the peaks are extremely broad or disappear completely, this indicates complete exfoliation.

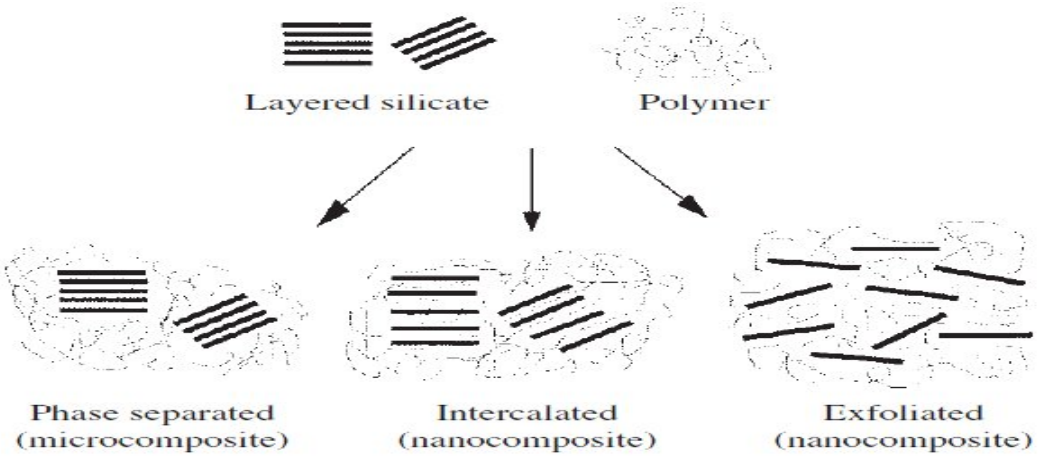

Fig.1.1. Three idealized structures of polymer-nanoclay composites[25]

1.4 Epoxy nanocomposites

In 1946, the first industrially-produced epoxy resin was introduced to market. Since then, the use of thermosetting polymers has steadily increased. The wide range of epoxy resin applications includes: coating, electrical, automotive, marine, aerospace and civil infrastructure as well as tool fabrication and pipes and vessels in the chemical industry. Due to their low density of around 1.3 g/cm and good adhesive and mechanical properties, epoxy resin became a promising material for high performance applications in the transport industry, usually in the form of composite materials such as fiber composite or in honeycomb structures. In the aerospace industry, epoxy-composites material can be found in various part of the body and structure of military and civil aircrafts, with the number of applications on the rise. A recent approach to improve and diversify polymer properties in the aerospace industries is through the dispersion of nanometer-scaled fillers in the polymer matrix. [Njuguna and Pielichowski, 2003]. A significant number of academic and industrial projects have investigated the possibilities to further improve epoxy

resin (and in some cases composites or other binary systems) through the strategy of producing nanocomposites.

The term ‘epoxy resin’ refers to both the polymer and its cured resin/hardener system. The former is a low molecular weight oligomer that contains one or more epoxy groups per molecule (more than one unit per molecule is required if the resultant material is to be cross-linked). The characteristic group, a three-member ring known as epoxy, epoxide, oxirane, glycidyl or ethoxyline group is highly strained and therefore very reactive. Epoxy resins can be cross-linked through a polymerization reaction with a hardener at room temperature or at elevated temperature (latent reaction). Curing agents used for room temperature cure are usually aliphatic amines, whilst commonly used higher temperature, higher performance hardener are aromatic amines and acid anhydrides. However, an increasing number of specialized curing agents, such as poly-functional amines, polybasic carboxylic acids, mercaptans and inorganic hardener are also used. All of these results in different, tailored properties of the final polymer matrix. In general, the higher temperature Cured resin systems have improved properties, such as higher glass transition temperatures, strength and stiffness, compared to those cured at room temperature.

1.5 Montmorillonite

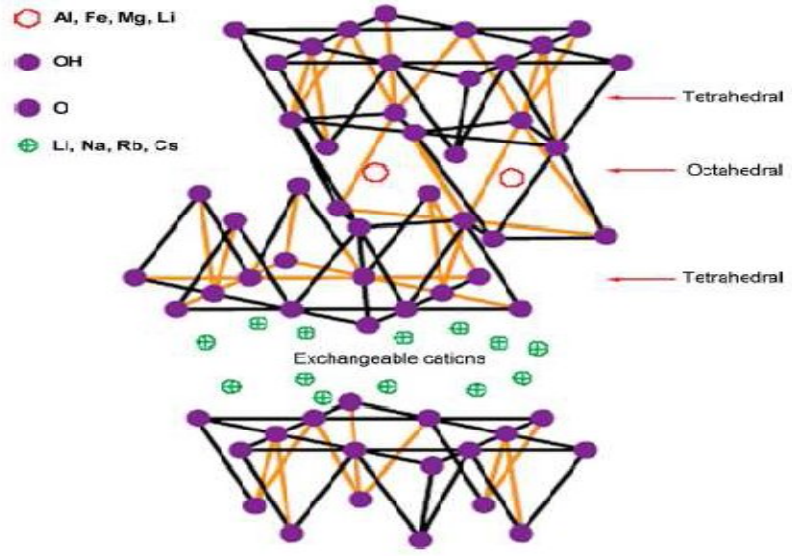

Fig 1.2 Structure of MMT[25]

One of the most widely used nanoclays is montmorillonite as shown at Figure 1.2. It has two silicate tetrahedral layers sandwiching an inner octahedral layer which consist of either alumina

or magnesia . The duty of the Na+ is to counterbalance the Al or Mg for generation of negative charge in the platelet. Montmorillonite has many platelets (layers), and there are Vander Waal forces between these layers . The gaps between the layers are called interlayer or gallery. For example, the X-ray d-spacing of completely dry sodium montmorillonite is 0.96 nm while the platelet itself is about 0.94 nm thick . The initial interlayer space is about 1.85 nm for Cloisite 30B®. Montmorillonite is in powder form with a mean particle size of about 8nm, and in each particle of powder there are more than 3000 platelets . The thickness of each layer is around 1nm, and the length of these layers can vary from 300Å to several microns i.e., it has high aspect ratio. Generally, there are two main considerations for polymer/layered silicate nanocomposites. The first one is dispersion of silicate particles into individual layers. The second is the ability of improving the surface chemistry through ion exchange reactions with organic and inorganic cations . Pretreatment of nanoclays using ammonium salts or alkyl phosphonium makes the nanoclays organophilic; the modified nanoclays are called organonanoclays . Figure 1.3 shows the exchange process between alkylammonium ions and metallic cations. After exchanging the ions, surface energy of inorganic host decreases and wetting properties of polymer matrix are improved. Larger interlayer spacing is obtained as a result

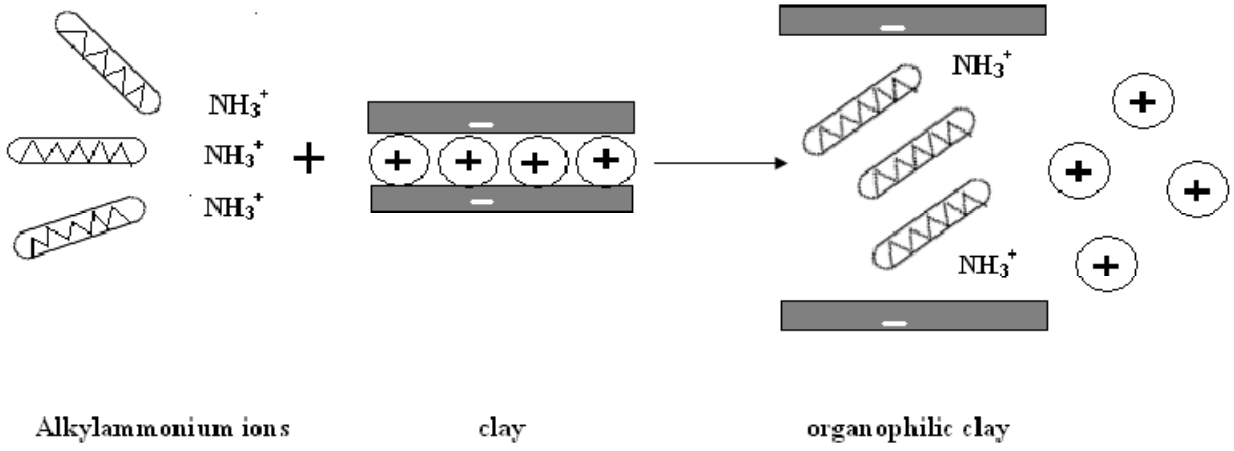

Fig 1.3 Exchange process between alkylammonium ions and metallic cations[25]

1.6 Glass fiber

Glass fiber is a material made from extremely fine fibers of glass, and it is the largest reinforcement measured in sales. Glass fiber was invented in 1938 by Russell Games Slayter of Owens-Corning as a material to be used as insulation (Lowenstein, 1973). Ever since then, glass fiber has become widely used as insulation and composite reinforcement material. Based on the composition and the application, glass fibers can be classified in several types.

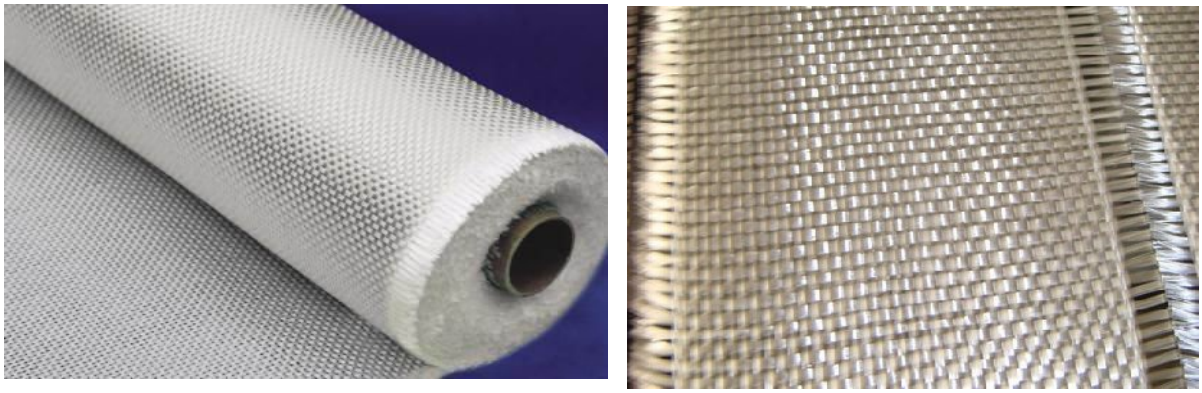

Fig. 1.4 Commercially available glass fibers [14]

The most commonly used glass fiber type for composite applications is E-glass, due to its relatively good mechanical properties and high electrical insulation. S-glass is also used in composite materials where high tensile strength is desired, however this material comes at a much higher cost. R-glass is also used in composite materials with high mechanical requirements such as fatigue life and high chemical resistance. The typical fiber diameter for glass fiber is 9-17 μm and the specific gravity is about 2.5. The tensile strength of glass fiber is in the order of 2000-4800 MPa and the elastic modulus is in the order of 50-90 GPa, much higher than that of polymers (Biron, 1973).

1.7 Carbon fiber

Carbon fiber is another major fiber reinforcement type used in FRPC. One of the most common methods of manufacturing carbon fiber is the oxidation and thermal pyrolysis of polyacrylonitrile (PAN), so called PAN-based carbon fibers. This material consists of extremely thin fibers about 5-10 μm in diameter and comprised mostly of carbon atoms. The carbon atoms are bonded together in microscopic crystals that are mostly aligned parallel to the long axis of the fiber. This

alignment makes the fiber show very high tensile properties. The tensile strength of carbon fiber is in the order of 3000-5800 MPa and the elastic modulus is in the order of 500-600 GPa (Lowenstein, 1973).

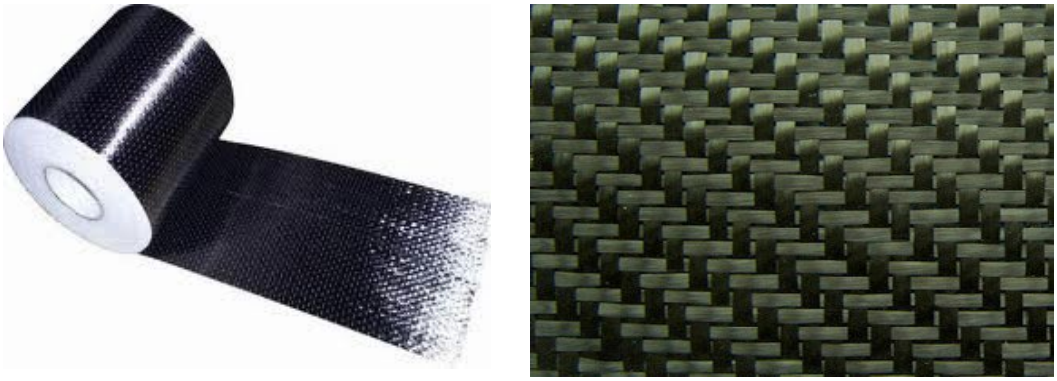

Fig. 1.5 Different types of matted carbon fibers[14]

Compared with glass fibers, carbon fibers have lower density but higher tensile strength and elastic modulus. These properties make carbon fiber an ideal reinforcement for composite materials used in aircraft components, high-performance vehicles, sporting equipment, wind generator blades, and other high demand, high performance applications.

1.8 Environmental effects on fiber composites

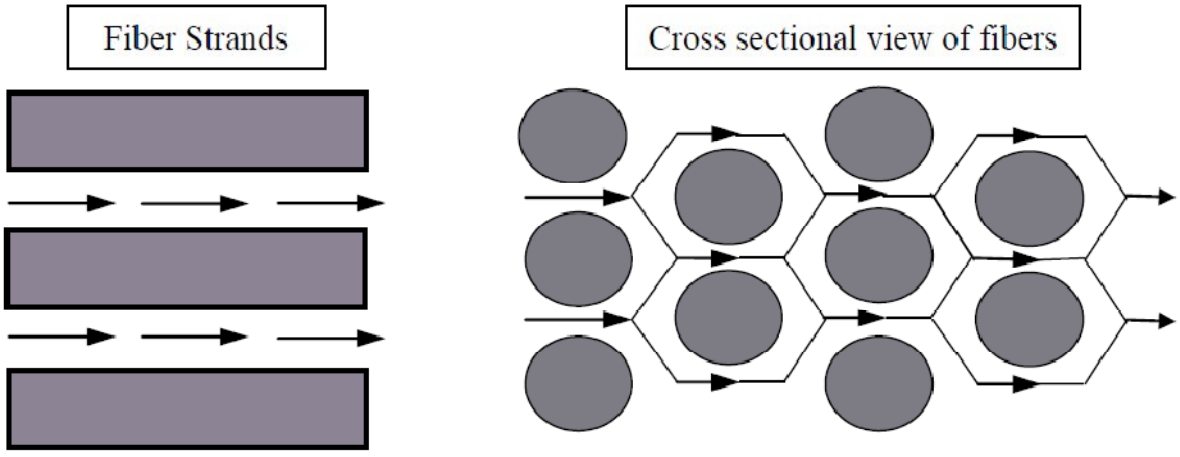

Fig. 1.6 Diffusion path of moisture into composite thickness direction[25]

Fibrous composites, especially carbon fiber reinforced epoxy are increasingly being used in military and aerospace applications owing to several desirable properties including high specific strength, high specific stiffness and controlled anisotropy. Despite these advantages over conventional structural materials such as metals, composites are susceptible to heat and moisture

when operating in harsh and changing environmental conditions. When exposed to humid environments, carbon–epoxy composites absorb moisture and undergo dilatational expansion. The presence of moisture and the stresses associated with moisture induced expansion can result in lowered damage tolerance, with an adverse effect on long-term structural durability. The amount of moisture absorbed by the epoxy matrix is significantly greater than that by the carbon fibers, which absorb very little or no moisture. This result in a significant mismatch in the moisture induced volumetric expansion between the matrix and the fibers.

In homogeneous materials, the kinetics of moisture diffusion is governed by the maximum moisture content and the diffusivity. The maximum moisture content is defined by the net amount of moisture that a fully saturated material contains under steady state equilibrium when exposed to a given environmental condition. It is usually expressed as the ratio of the increase in weight per unit dry weight at the point of saturation. The relative weight gain approaches the maximum moisture content of composite at infinite time. It has been shown that the maximum moisture content strongly depends on the relative humidity of the exposure environment. Usually the maximum moisture content is determined by exposing the material to a humid environment for a long duration of time until steady state equilibrium is attained. This process often takes several months, which makes the procedure cumbersome and time consuming. Also the rate of moisture diffusion is governed by the diffusivity. In general, the diffusivity is a strong function of the ambient temperature and a weak function of the relative humidity. In the case of composites, the diffusion process is more complex. It depends on the diffusivities of the individual constituents, their relative volume fractions, constituent arrangement and morphology. Traditionally, effective diffusivity has been used to predict the amount of moisture content. The figure 1.7 shows the various effects of moisture diffusion on a composite sample. When a fiber-reinforced composite material is exposed to a hygrothermal environment and mechanical loads, changes in material properties are expected. These changes in material properties are connected to an irreversible material degradation. The moisture may affect the laminates through chemical changes such as relaxation and oxidation of the matrix material. A cyclic moisture environment exposed laminate experience damage such as debonding at fiber/matrix interfaces and continuous cracks. Usually one of the first observed damage modes in a laminated composite is *matrix cracking*. These cracks are in general not critical for final failure, but if they are connected to a surrounding moisture environment more rapid moisture absorption may be

expected for the cracked laminate. The accelerated moisture absorption in a cracked material exposed to humid air is a result of the faster diffusion in air compared to the diffusion speed in the composite material. Faster moisture uptake may also develop a faster material degradation. This makes it important to know the moisture absorption behavior in a cracked laminate.

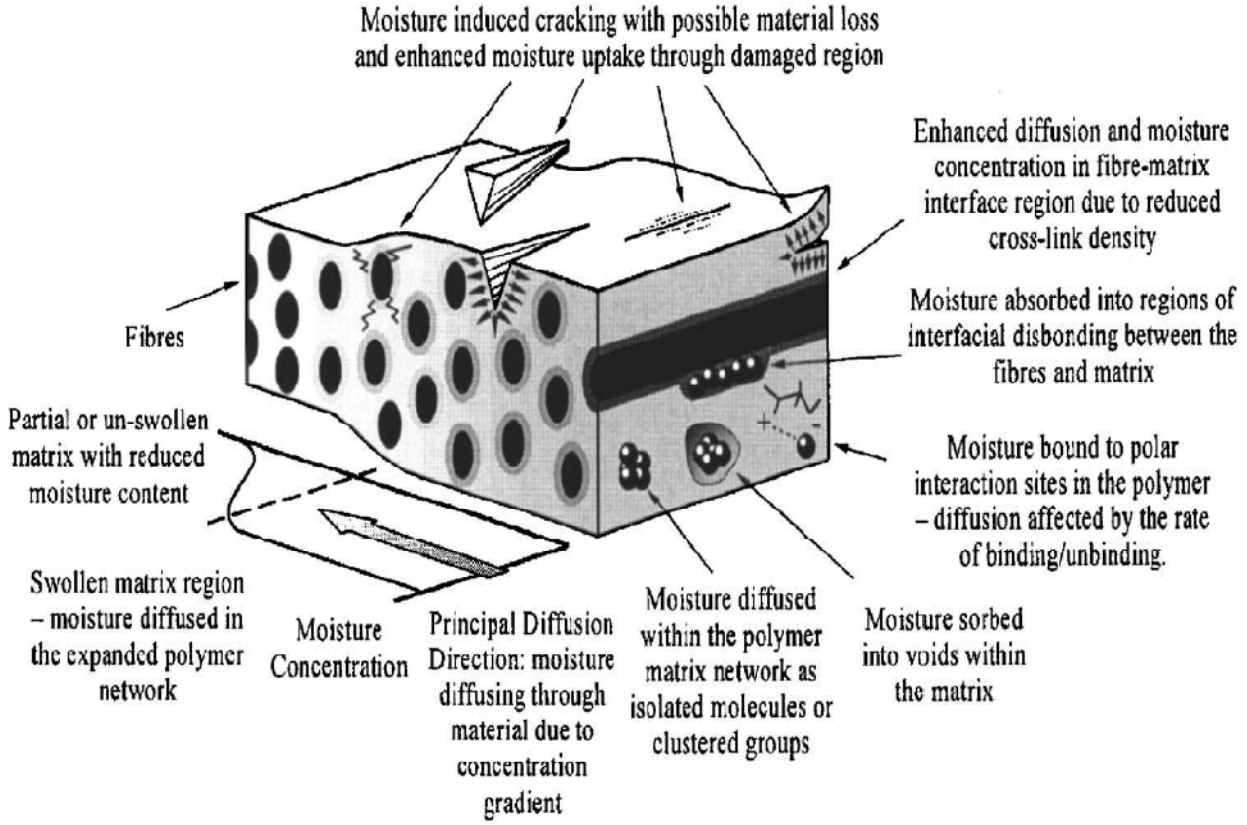

Fig. 1.7 Deteriorated fiber specimens under moist environmental condition[25]

For an undamaged material, well-accepted moisture transportation models are available. The most common models for the transportation of moisture in undamaged polymeric composite materials are Fickian diffusion and Langmuir diffusion. If the material contains cracks that significantly affect the moisture uptake, then the original laws of Fickian and Langmuir are no longer valid for the whole laminate, but locally they still work. The influences of matrix cracks on moisture uptake in glass-fiber/epoxy laminates have been studied. Experiments, finiteelement calculations and analytical calculations have been performed and the results are compared. The experimental results show that crack closure may occur early in the absorption process and that the crack closure is significantly influencing the moisture absorption.

Extensive literature review has been carried out for defining the research problem. Most of the work carried out is on the characterization of composites by addition of nanoclay to matrix system. GFRP with postcuring and their environmental degradation under different conditions has not been addressed so far.

Wang *et al.* (2001) prepared polymeric nano-composites by melt intercalation method. The nanoclay was mixed with polymer by twin-screw extrusion. The nanoclay-spacing in the composites was measured by X-ray diffraction (XRD). The morphology of the composites and its development during the extrusion process were observed by scanning electron microscopy **(**SEM**).** Melt viscosity and mechanical properties of the composites and the blends were also measured. It was found that the nanoclay spacing in the composites was influenced greatly by the type of polymer used. Also the addition of the nanoclay increased the viscosity of the polymer when there was a strong interaction between the polymer and the nanoclay. The mechanical test showed that the addition of 5-10 wt.% nano-nanoclay largely increased the elastic modulus of the composites. The water absorption of nylon 6 was decreased with the presence of nano-nanoclay. The effect of nano-nanoclay on polymers and polymer blends was also compared with Kaolin nanoclay under the same experimental conditions.

Sinha Ray *et al.* (2003) discussed the academic and industrial aspects of the preparation, characterization, materials properties, crystallization behavior, melt rheology and processing of polymer/layered silicate nanocomposites. Smectites were a valuable mineral class for industrial applications because of their high cation exchange capacities, surface area, surface reactivity, adsorptive properties. These composites exhibited improved mechanical properties compared to conventional composites. The composites exhibited a remarkable increase in thermal stability, as well as self-extinguishing characteristics for flammability, such that the flammability of pristine polymers were significantly reduced after nanocomposite formation with layered silicate.

Petre (2004) discussed the difference between the properties of the material that changed after postcuring of the material and found that the strength of the postcured material was significantly

higher than the material that are cured at normal temperature which is due to the better crosslinking of the polymer.

Chow *et al*. (2005) analysed the water absorption and hygrothermal aging behaviour of organomontmoiillonite (OMMT reinforced polyamide 6/polypropylene (PA6/PP ratio = 70/30), with and without maleated PP (MAH-g-PP), at three different temperatures (30, 60, and 90^{o}C. The water absorption of the PA6/PP nanocomposites obeyed the Fickian law behavior. It was found that the equilibrium moisture content and the diffusion coefficients were dependent on the OMMT loading, MAH-g-PP concentration and immersion temperature tensile modulus and strength of PA6/PP nanocomposites deteriorated after exposure to hygrothermal aging. Water acted as a plasticizer for the PA6/PP matrix and silicate layer of OMMT. The nanocomposites showed excellent retention ability and recovery properties under any immersion temperature. The MAH-g-pp enhanced the resistance of the nanocomposites against water immersion and also improved the resistance against hygrothermal attack.

Kornmann *et al*. (2005) synthesized and successfully used epoxy-layered silicate nanocomposites based on anhydride cured epoxy and octadecylamine modified fluorohectorite as matrix in glass-fiber-reinforced laminates by hand lay-up technique. The material used was the synthetic layered silicate Somasif ME-100. One hundred and twenty milli-equivalents per 100 g of Somasif ME-100 of ocadecylamine were dispersed in deionised water at 80^{o}C. Flexural tests had been performed on the laminates and indicated that the presence of silicate layers in the epoxy matrix leads to a flexural strength improvement of 27%. According to dynamic mechanical measurements, the presence of organosilicate caused a decrease of the glass transition temperature. The glass transition temperature decrease was apparently responsible for the larger water uptake observed in the nanocomposite.

Lin *et al*. (2005) prepared Layered silicate/glass fiber/epoxy hybrid composites using vacuum-assisted resin transfer molding (VARTM) process. Unidirectional glass fibers were placed in two directions: parallel and perpendicular to the resin flow direction. The intercalation behavior of the nanoclay and the morphology of the composites were investigated using X-ray diffraction (XRD) and transmission electron microscopy (TEM). The complementary use XRD and TEM techniques revealed an intercalated nanoclay structure in the composites. Dispersion of nanoclay in the composites was also observed using scanning electron microscopy (SEM); the observed

nanoclays were dispersed between both the bundles of glass fibers and within the interstices of the fiber filaments. The mechanical properties of the ternary composites were evaluated. The results indicated that introducing a small amount of organonanoclay to the glass fiber/epoxy composites enhanced their mechanical and thermal properties, confirming the synergistic effects of glass fibers and nanoclays in the composites.

Chowdhury *et al.*(2006) carried out a systematic study to analyse the effect of nanoclay amount on the tensile and flexural properties of the woven carbon fiber reinforced polymer composite and difference in the properties that occur if the cured material is further thermally postcured and concluded in the end that thermally postcured material have some increase in the strength.

Yasmin *et al.* (2006) prepared the nanoclay/epoxy nanocomposites by shear mixing method and used the 1-10wt. % of nanoclay concentration to prepare the samples. The epoxy matrix was reinforced with MMT nanoclay particles to fabricate nanoclay/epoxy nanocomposites. They used bisphenol A as epoxy resin and methyl tetrahydrophthalic anhydride as the hardener. Two types of nanoclay nanoparticles were used as the reinforcement, one was Nanomer I.28E and other was Cloisite 30B. In this study Closite 30B showed a homogeneous dispersion of nanoparticles throughout the cross-section compared to Nanomer I.28E/epoxy. As the nanoclay content increased, the strain to failure decreased. It was also found that the modulus of the nano-composites increased monotonically with increasing nanoclay content. For 10wt.% of nanoclay, the Cloisite30B/epoxy showed an increase of 53% over the neat resin, where as the other showed an increase of about 22% at room temperature. The observation further confirmed the direct relation between the degree of exfoliation and the mechanical properties of these nanocomposites. The addition of nanoclay also found to reduce the CTE (coefficient of thermal expansion) of pure epoxy.

Avila *et al.* (2006) prepared a set of fiber glass-epoxy-nanoclay laminate composites to investigate how the plate impact strength is affected by the presence of nanoclays. The S2-glass/epoxy-nanoclay composite made was a laminate with 16 layers and 65% fiber volume fraction prepared using a vacuum assisted lay-up technique. The amount of nanoclay added into an epoxy system, in weight, was 1%, 2%, 5%, 10%, respectively. To compare the results, a set of S2-glass/epoxy laminated composites were also prepared. The addition of nanosized nanoclays increased the composite impact strength, as the damaged area was decreased approximately 20%

for small amounts of nanoclay contents. When the concentration reached around 10% the increase on impact strength was near to 50%. Nanoclay composites showed great performance over the conventional composites under the rebound/spring effect. When the four edge clamped condition was imposed the overall composite damping was increased with the nanoclay concentration. The most favourable nanoclay concentration suggested by them was close to be 5%. This could be due to the vibration mode superposition associated to a stiffness enhancement.

Avila *et al.* (2006) investigated the influence of montmorillonite (MMT) silicate layers on glass-fiber-epoxy laminated composites behavior by low-velocity impact and X-ray diffraction tests. The nanostructure laminate prepared for the investigation was a S2-glass/epoxy-nanoclay. The nanoclay used was Nanomer I30E. The amount of nanoclay dispersed into the epoxy system, in weight, was 1%, 2%, 5%, 10%, respectively. As the amount of nanoclay dispersed was increased, there was an increase in stiffness. As the stiffness reached its peak value, the fracture toughness and damping were reduced. Specimens with 5% nanoclay content showed the best performance with respect to damping. As the energy increased, the nanostructure laminate response got weaker. When the low-velocity impact results were analyzed they showed an increase on energy absorption close to 48% for low energies, 20 J, 15% increase for medium–high energies, 60 J, and 4% for high energy, 80 J. As the amount of intercalated nanoclay content varied from 0% to 10%, the optimum condition for low-velocity impact seemed to be around 5%.

Wetzel *et al.* (2006) analysed the manufacturing and the characterization of epoxy nanocomposites. Special attention was directed towards reinforcing effects of nanoparticles on the polymer toughness. The incorporation of both Al_2O_3 and TiO_2 nanoparticles into the epoxy resin improved flexural stiffness, flexural strength, and fracture toughness of the polymer at the same time. Cracks in Dynamically loaded nanocomposites propagated at lower rates than in neat epoxy. The fillers were well bonded to the matrix, which was indicated by both the shift of the glass transition temperature to higher temperatures and the increase in the rubbery plateau modulus. Moreover, the presence of Al_2O_3 in epoxy increased the apparent yield stress, the yield strain, and the size of the plastic zone. Debonding effects in the process zone, as often observed in glass bead filled epoxies, were rather unlikely to participate in the toughening of EP/Al_2O_3 nanocomposites, due to the small dimensions of fillers. Further investigations would help to find

relationships especially between the morphology, the relevant toughening mechanisms, and the toughness of EP/Al_2O_3 nanocomposites. It was believed that the observed property characteristics were related to the influence of nanoparticles on the molecular structure of the matrix itself.

Wang *et al.* (2006) investigated the effects of hydrothermal ageing on the thermo-mechanical properties of high performance epoxy and its nanocomposite. In this work epoxy–nanoclay nanocomposite samples containing 2.5 wt% of nanoclay were prepared through a "slurry-compounding" approach. The cured samples were immersed in distilled water at 60°C for different periods of time before subjecting to characterization. The hydrothermal effect on the thermal/mechanical properties of neat epoxy and epoxy–nanoclay nanocomposite was studied. The moisture uptake significantly affects the modulus at high temperature, the tensile strength, and the α-relaxation behavior. On the other hand, at low temperature, the modulus and fracture toughness were not strongly influenced. As the moisture content increased, there was a reduction in strain at break for the epoxy–nanoclay nanocomposite while that of the neat epoxy remained constant. This effect was attributed to epoxy–nanoclay interface debonding induced by water and formation of water cluster fillers that acted as defects in the composite.

Berketis *et al.* (2007) investigated the matrix and fiber/matrix interfacial degradation of glass fiber composites subjected to water for very long time. Laminated composite plates were manufactured by the vacuum assisted resin transfer moulding technique. The resin used was the polyester (crystic 489 PA). Durability of an isopthalic polyester resin reinforced with non-crimp glass fabrics in a hydrothermal environment for up to 30 months was observed. The weight of the composite plates initially increased due to water diffusion up to month 14 and thereafter decreased due to material losses. The initial weight increase was due to diffusion of water into the specimens. Immersion in water also resulted in significant de-bonding of the fiber/matrix interface, which allows water to penetrate the composite material by capillary action. The impacted plates were retested statically to determine residual compressive strengths for the assessment of damage tolerance. A new device was designed for the CAI tests that assured laminate failure by de-lamination propagation. The results of the CAI testing demonstrated a reduction in CAI strength, due to hydrothermal exposure for each applied level of impact

loading. Immersion time of 24 and 30 months showed that a local plateau was approached in CAI strength.

Quaresimin *et al*. (2007) analysed the effect of three different commercially available nano-modifiers on the mechanical properties of an epoxy/anhydride unidirectional carbon fiber reinforced laminates. The polymeric matrix consisted of a blend of the diglycidyl ether of Bisphenol A and the epoxy novolac resin. The hardener was a hexa-hydrophthalic anhydride. The nanoclay used was Cloisite 30B. The organonanoclay was dispersed through a shear mixing process. Hand-layup method was used to prepare the specimens. The tensile modulus exhibited little difference between the unmodified laminates while a modest decrease was observed for the tensile strength for the VGCF (vapors grown carbon fiber) and nanoclay modified systems.

Shang-Lin *et al.* (2007) performed experimental investigation of nanocomposite coatings for healing surface flaws of glass fibers and improving alkali-resistance. He found that, with low fraction of nano-reinforcements, the nanostructures and functionalised traditional glass fibers show significantly improved both mechanical properties and environmental corrosion resistance. The most remarkable mechanical strength improvement was found for glass fibers with nanotube coatings, corresponding to the highest healing efficiency factor. No apparent strength variation appeared for nanoclay coated fiber subjected to alkaline attack, which indicated that, the influence of moisture solvent uptake and concentration on mechanical properties decreased when the organonanoclay was dispersed in coating polymer. Overall, the hybrid nanocoatings caused improved fiber strength, corrosion resistance, and interfacial properties.

Chow *et al. (2007)* prepared the epoxy/glass fiber/organo-montmorillonite (OMMT) nanocomposites by hand lay-up method. In this work, the epoxy nanocomposites were characterized by X-ray diffraction (XRD), differential scanning calorimetry (DSC) and water absorption tests. Epoxy/glass fiber/OMMT hybrid nanocomposites prepared by hand-layup technique showed exfoliation characteristics and slightly enhancement in glass transition temperature. The water resistance properties of epoxy were improved by the addition of both glass fiber and OMMT, which is may be attributed to the increasing of the tortuosity path for water penetration.

Manjunatha *et al.* (2009) investigated the tensile fatigue behavior of a silica nanoparticle-modified glass fiber reinforced epoxy composite. The epoxy resin was a standard diglycidyl of Bisphenol A with an epoxide. The GFRP composite laminates were manufactured by resin infusion under flexible tooling technique. An anhydride-cured thermosetting epoxy polymer was modified by incorporating 10 wt. % of well-dispersed silica nanoparticles. The fatigue life of 10 wt. % silica nanoparticle-modified bulk epoxy was about three to four times higher than that of neat epoxy. The fatigue life of the GFRP composite with 10 wt.% silica nanoparticle modified epoxy matrix was about three to four times more than that of the GFRP with the neat epoxy matrix. The suppressed matrix cracking and reduced crack growth rate due to the particle debonding and plastic void growth mechanisms appeared to contribute for the observed enhancement of the fatigue life in the GFRP with the nanoparticle-modified matrix.

Maitra *et al.* (2009) synthesized and evaluated PVA polymer-matrix composites reinforced with small concentrations of functionalized ND. Detailed structural characterization, employing a variety of analytical techniques, showed that the nanoparticles were distributed uniformly and did not agglomerate. Further, they appeared to interact with the polymer matrix strongly, increasing the crystallinity substantially. The mechanical properties of the PVA-ND composites were determined using nano-indentation technique. With only 0.6-wt% addition of ND, which was relatively small, significant enhancements to the hardness and Young's modulus of the PVA were observed. It was suggested that excellent adhesion between the matrix and the functionalized ND particles was the main reason for this marked improvement in mechanical performance. These results indicated that ND could be successfully used as a filler material for making polymer composites.

Zainuddin *et al.* (2010) analysed the effect of environmental conditioning especially under hot-wet conditions on E-glass epoxy fiber reinforced composite. The weight gain was higher for all the wet conditions samples exposed to elevated temperatures. Addition of 1–2 wt% of nanoclay decreased the weight gain. Flexural properties were found to degrade with increase in time. 2 wt% GFRP composites showed enhancement in properties under all conditions over neat counterparts. In some cases, samples subjected to hot dry condition at 60^0C showed increase in properties over room temperature conditioned samples. Scanning electron micrographs provided clear evidence of the effects of nanoclay, elevated temperature and moisture absorption.

Enhancement in interfacial bonding was observed in 2wt.% composite samples, both at room temperature and hot-wet conditioning.

Hossain *et al.* (2011) investigated the effect of seawater on the degradation of mechanical properties of conventional and nanophased carbon-epoxy composites. Epoxy resin was modified using 1 wt.%, 2 wt.%, and 3 wt.% nanoclay. Carbon-epoxy composites were fabricated by vacuum assisted resin transfer molding process and compared with neat samples with and without exposure to seawater. Nanoclay was dispersed into matrix by using magnetic stirring. Mechanical characterization performed through three point bending tests showed that 2 wt.% nanoclay loading was optimum. Flexural strength and modulus were increased by 25% and 12.51%, respectively, compared to neat system for samples not exposed to seawater. Flexure samples exposed to the seawater for 30, 60, and 180-day periods revealed that samples with nanoclay retained better mechanical properties compared to neat samples. After 30-day exposure to seawater, there was no significant reduction in the strength and modulus. However, flexural strength was reduced by 10.24%, 7.08%, 5.28%, and 7.13% for neat, 1 wt.%, 2 wt.%, and 3 wt.% nanoclay-infused samples, respectively, after the samples were exposed to seawater for 180-day. At the same time flexural modulus was reduced by 12.61%, 7.16%, 4.59%, and 6.11%, respectively. From scanning electron microscopy (SEM) studies, it was found that failure occurred due to delimitation and initiated from the compression side. Nanophased composites exhibited better bonding between fiber and matrix. SEM micrographs also revealed that both unconditioned and conditioned nanophased epoxy, which produce relatively rougher fracture surfaces compared to neat samples. Optical microscopy study revealed no significant physical change in outer surfaces of the samples conditioned up to a 90-day period.

Zafar *et al.* (2012) investigated the long term effects of moisture on the interface between a carbon fibre and an epoxy matrix. High modulus carbon fibres were used to prepare single fibre model composites based on an epoxy resin. The samples were immersed in the seawater and demineralised water and their moisture uptake behaviour was monitored. The equilibrium moisture content and diffusion coefficients for the samples were determined. DSC (Differential scanning calorimetry) has been used to analyse the moisture effects on glass transition temperature and thermal stability of the pure epoxy specimens. These results showed a reduction in the glass transition temperature (Tg) after moisture absorption. Tensile tests were also carried

out for the epoxy specimens and a general decrease in the mechanical properties of the epoxy matrix was observed. Raman spectroscopy was used to observe the effects of moisture on the axial strain of the carbon fibre within the composite and stress transfer at the interface as a function of exposure time. The results show that the decrease in the mechanical and interfacial properties of the model composites under the seawater immersion is more significant than under demineralised water immersion.

CHAPTER 3 GAPS IN LITERATURE

3.1 Gaps in literature

Earlier literature review depicts that work has been mainly focused on the synthesis of polymer nanocomposites and the characterization of the mechanical properties. There are no detailed studies on curing process of epoxy matrix for preparing FRPs and then carrying out the hygrothermal studies. Some of the following gaps in the previous research are: Still fewer reports are there on the use of nanocomposites as matrix in fiber-reinforced composites for curing studies.

1. There is no work done on changing the curing technique.
2. Most of the work is focused on the synthesis and characterization and not on hygrothermal aging studies of nanocomposite epoxy based FRP.

3.2 Research problem

The present study is mainly focused upon the influence of postcuring and nanoclay content on the mechanical properties. In this study, mechanical properties and thermal stability of these FRP laminated nanocomposites with different curing techniques. It is also proposed to carry out some hygrothermal aging studies on these FRP.

4.1 Work plan

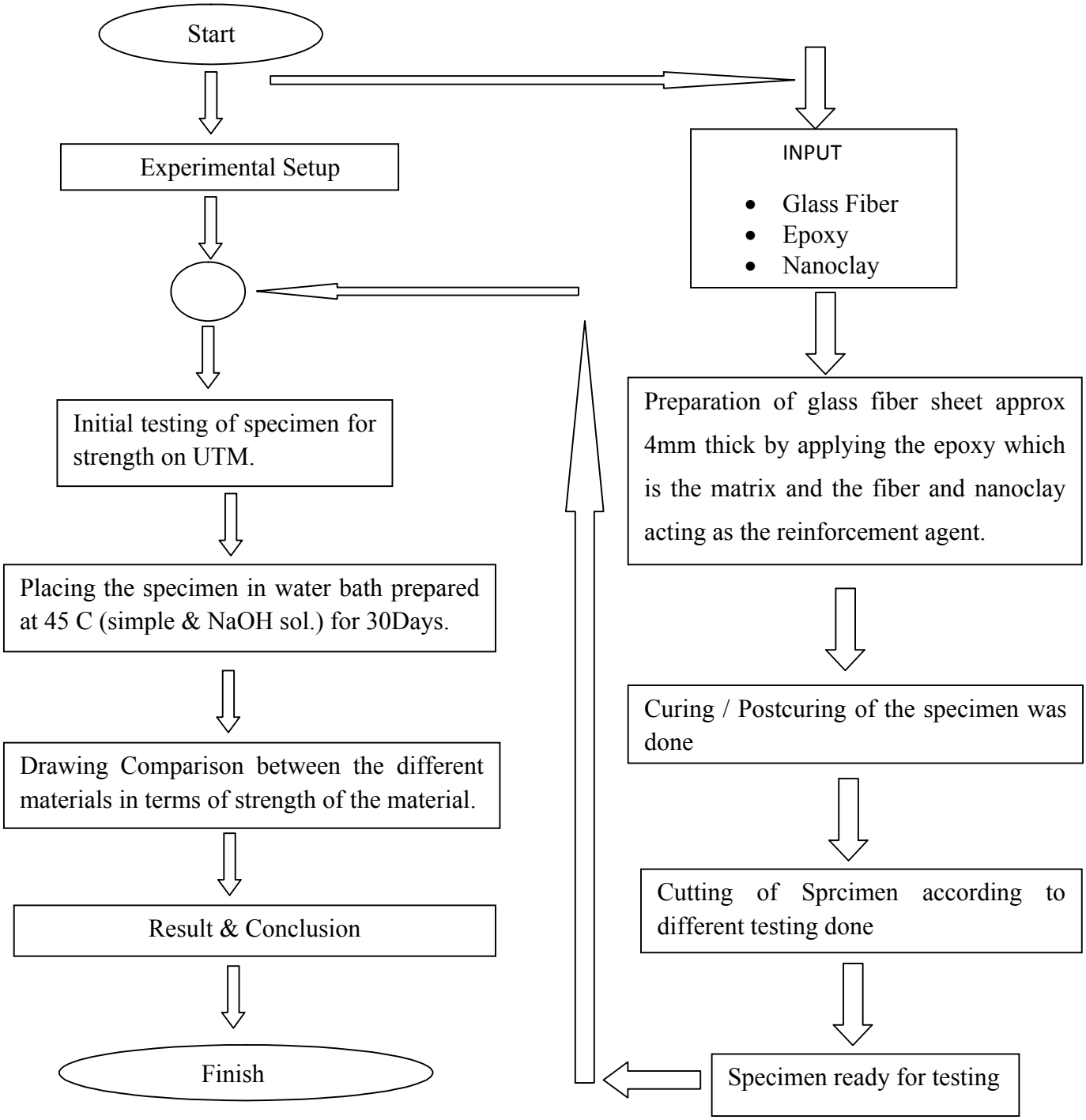

Fig 4.1 Plan of the work

4.2 Fabrication of specimen

4.2.1 Materials & apparatus used

Unidirectional E-glass fiber and M Brace a two part epoxy resin was purchased from **BASF Construction Chemicals (India) Private Limited**. Organically modified nanoclay Closite 30B® was purchased from **Connell Bros. Mumbai. JULABO REMI** Stirrer , precision **OIL BATH** and **ULTRASONIC BATH** were used in the processing.

4.2.2 Specimen specifications

Commercially available glass fiber mat had been used for making specimen. The sheets were placed along 0^0 orientation side for cutting the specimen. The specimen had been cut and prepared as per the testing standards for tensile(DIN EN ISO 527-4) and bending tests(DIN EN ISO 14125) respectively. The dimensions of specimens are shown below.

Table 4.1 Specimen specifications for testing

Parameters for Specimen	Specimens for tensile testing	Specimens for Flexural testing
Length	125 mm	125 mm
Width	15 mm	13 mm
Thickness	4 mm	4 mm

4.2.2.1 Specimen dimensions

- **For bending test**

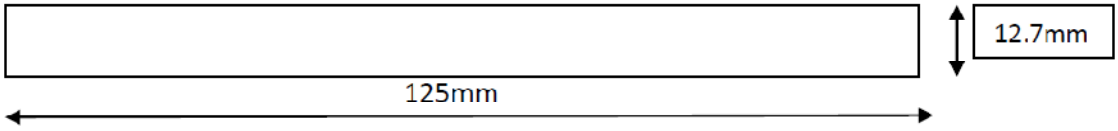

Fig.4.2(a) Specimen dimensions for bending test

- **For tensile test**

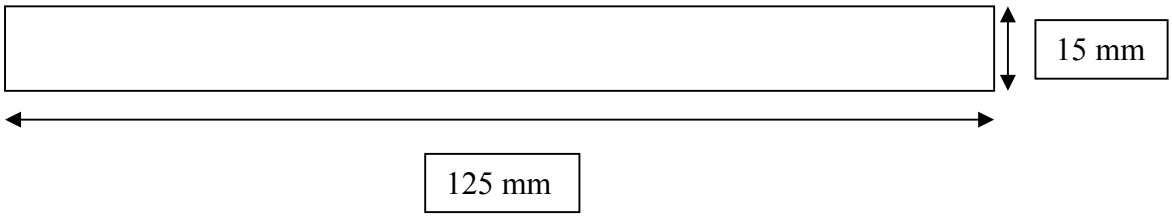

Fig.4.2(b) Specimen dimensions for tensile test

4.2.3 Cutting glass fiber sheet

For the experimentation unidirectional roll of glass fiber was purchased having 50 cm width having 0^o fiber orientation woven with polymer fibers. The sheets were initially cut from roll in lengths of 250 mm.

Fig 4.3 Uncoated glass fiber mat

4.2.4 Mixing of nanoclay into epoxy (base):

- **Mechanical stirring**: Epoxy base is a blue colour thick fluid. It is quite difficult to mix nano silicates into it manually. Mechanical stirrer and an oil bath is used for proper mixing of nanoclay Oil bath was used to heat up the epoxy to desired (60^0C) temperature, so that the viscosity of epoxy base is reduced.

Fig. 4.4 Oil bath set-up with mechanical stirrer

Proper mechanical stirring of epoxy at this stage resulted in a better dispersion of nanoclay. Different weight percentages of nanoclay i.e. 0.5, 2, 3 and 4 % by weight of epoxy, were added and stirred at a temperature of 60^0C for 2 hours.

- **Ultrasonication after mechanical stirring:** Sonication is the act of applying sound energy to agitate particles in a sample, for various purposes. In the laboratory, it is usually carried out using an ultrasonic bath or an ultrasonic probe, colloquially known as a sonicator. Sonication can be used to speed dissolution, by breaking intermolecular interactions. Sonication was done for evenly dispersing nanoparticles in liquids. After mechanical stirring of the epoxy solution container was placed into the ultrasonication bath for up to 2 hours.

Fig4.5 Ultrasonic bath

4.2.5 Mixing of epoxy base solution with hardener:

After ultrasonication, the solution is mixed with the hardener in the ratio 5:2 by volume. After mixing, stirring up to 5 to 10 minutes was done.

Fig4.6 Mixing of hardner and base

4.2.6 Coating of nanoclay mixed epoxy to glass fiber sheets:

The mixture was then poured on to the glass fiber mat and applied uniformly using the hand layup method. For this a steel scraper was used to maintain uniformity of the applied solution. It was ensured that there were no air bubbles entrapped inside the epoxy applied on sheet otherwise it would create a flaw there. These sheets i.e. I, II & III, were prepared for each composition. The full curing of sheet I and III was done by leaving it at ambient temperature (28^0-30^0) for at least 12 hours before processing further.

4.2.7 Curing of the prepared sample

Sheet I is cured at ambient temperature and sheet II was immediately put in the vaccum oven at temperature 100^0 C for 5 hours and allowing it to cure inside the oven. Similar heating of sheet III was done after curing it at room temp(it is combination of both I&II).

Fig4.7 Vaccum oven

4.2.8 Sizing of sheet for samples

Once the epoxy was fully cured, cut the sheet to actual sample size using the marble cutting machine.

Fig 4.8 Marble cutter

4.3 Experimental set-up

A set of accelerated aging tests had been carried out to evaluate performance of glass fiber reinforced polymer (GFRP) sheets embedded in epoxy matrix. The field environment very similar to that of tropical climate had been simulated. The specimens were immersed in two water baths for different time durations.

Fig. 4.9 Setup view of the water baths

The specimens were removed from the bath after an interval of 30 days. The tensile and flexural strength was measured to check the degradation in properties of composite material. Both of the water tanks were filled with water. One was of simple water and other tank was containing 5% NaOH by weight of water. Both the tanks were kept at a temperature of 45^0C.

4.3.1 Setup fabrication:

Table 4.2 The set-up basically consists of following main components

S.No.	ITEM NAME	QUANTITY
1	Water tanks	02
2	Specimens	96
3	Heating Elements	02
4	RTD Sensors	02
5	Temperature Controllers	02

4.3.2 Water Tanks:

The experimental setup consists of two well insulated tanks (Fig. 4.9). The tank was of cylindrical shape made out of plastic. The approximate capacity of the tank was 60 l. Both the tanks were filled totally with tap water and set at a temperature of 45°C. NaOH was added to one tank (5% by weight of water). The water which evaporated from the tank was replenished on daily basis during experimentation. Each tank was labeled as per details of experimentation.

4.3.3 Heating Element:

The setup was heated with help of commercially available heating rod elements (Fig. 4.10). Each bath was having its own heating rod connected via temperature controller (Fig.4.11). The wattage of rod was 1000 KW with single phase connection. As the temperature reached the required value the power supply of rods were cut off by PID controllers.

Fig. 4.10 Heating Element and RTD sensor in a tank

4.3.4 Temperature Controller:

The objective of this set up was to maintain the bath temperature at specified value till the duration of experiment for day and night on daily basis. So a temperature controller (Fig.4.11) was connected with each of the bath along with relays cut off. The controller used the proportional-integral-derivative (PID) control to maintain the temperature. On the controller display the “Set Value” was given which was the temperature indicated in green and the “Process Value” of temperature was indicated in the red (refer Fig.4.11), which was the output from the RTD sensor. For the very first time the controller was set to auto-tune mode so that it could adjust itself according to the input variables. Once the bath had attained the set value the

controller cut off its supply and after sometime it sensed the temperature if it had gone below set value, it again started heating to obtain the set value.

Fig. 4.11 Temperature controller **Fig. 4.12 Temperature display panel with controller**

4.4 Testing methods used in experimentation

4.4.1. Tensile testing

A Universal Tensile Testing machine shown in Fig. 4.13 and Fig. 4.14 was used for the testing of the FRP specimen for determining its tensile strength. The test specimen had been prepared according to assumed dimensions. The specimen were tested until they break indicating the peak load and ultimate stress value they can bear at required time period to estimate the degradation in the same machine.

Fig. 4.13 UTM testing machine **Fig. 4.14 Specimen in jaws**

4.4.2. Three point flexural Test

Three point bending tests of specimen were carried out in using Zwick/Roell (Fig. 4.15 & Fig. 4.16).

Fig. 4.15 Three point bend test machine **Fig. 4.16 Specimen positioning**

The test specimen had been prepared according to standards. The three point bending test results can be taken as indications of strength degradation of composites after they had been hygrothermally treated.

4.4.3. Micro hardness test

Micro hardness test (shown in Fig. 4.17) was conducted on specimen with different nanoclay loadings to see the effect of nanoclay loading on hardness values.

Fig. 4.17 Micro hardness testing equipment

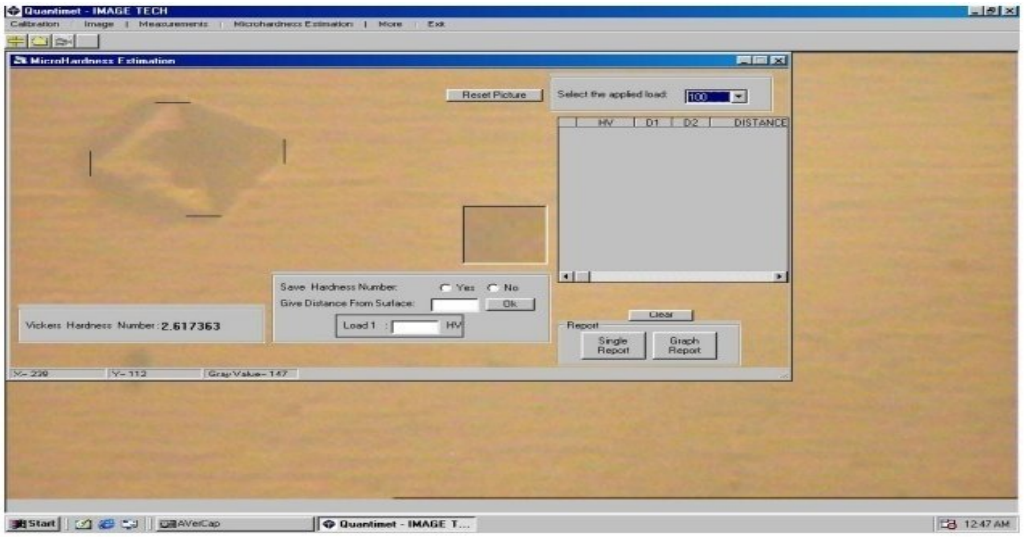

Fig. 4.18 Indent of specimen

The load applied was 50gm and VHN values were determined by applying this load by using a calibration distance of 50 units in Quantinet software as shown in Fig.4.18 used for image analyzing. The dwell time used during load application was 20 seconds. An indent is formed in diamond shape used for calculating VHN as shown in figure.

4.4.4. X-ray diffraction test

X-ray scattering techniques are a family of non-destructive analytical techniques which reveal information about the crystallographic structure, chemical composition, and physical properties of materials and thin films. These techniques are based on observing the scattered intensity of an X-ray beam hitting a sample as a function of incident and scattered angle, polarization, and wavelength or energy.

X-ray diffraction was used in this study to investigate the crystallographic structure of the epoxy nanocomposites. XRD will enable the changes that occur to the nanoclay due to the intercalation and/or exfoliation of the epoxy into the nanoclay galleries to be quantified. The d-spacing of the intergallery spacing can be determined using Bragg‟s Law:

$$\lambda = 2d\sin\theta$$

Where λ is the wavelength of the incidence x-ray source, d is the spacing in question, θ is ½ of 2θ the Bragg angle or the diffracted angle of the incidence x-ray beam. Below is a schematic of the previously mentioned Bragg's Law (Fig. 4.19).

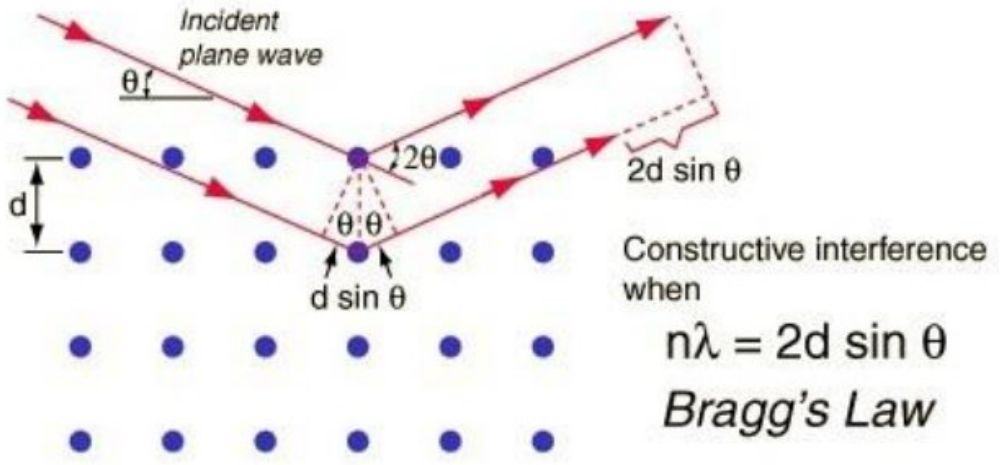

Fig. 4.19 Schematic representation of x-ray diffraction principle and the bragg's law

To evaluate the degree of exfoliation in the polymer, XRD measurements were carried out in a Panalytical X-ray diffractometer with Cu Kα radiation (λ=1.54Å) with a scanning speed of 10/min and at 45 kV and 40mA. During the XRD experiments, the samples were analyzed in reflection mode. All XRD scans were through 2θ of 5^0 to 15^0.

4.5 Test matrices

Table 4.3 Initial testing specimens

Specimen Name	No. of specimens						Total specimens
	Normally Cured		Cured at 100^0C		Postcured		
	Tensile	Bending	Tensile	Bending	Tensile	Bending	
0.5 wt%	2	2	2	2	2	2	12
2 wt%	2	2	2	2	2	2	12
3 wt%	2	2	2	2	2	2	12
4 wt%	2	2	2	2	2	2	12
	Total specimens						48

Table 4.4 Distribution of above GFRP nanocomposite specimen for accelerated degradation in 45°C Simple Water Bath

Specimen name	No. of specimens						Total specimens
	Normally Cured		Cured at 100^0C		Postcured		
	Tensile	Bending	Tensile	Bending	Tensile	Bending	
0.5 wt%	2	2	2	2	2	2	12
2 wt%	2	2	2	2	2	2	12
3 wt%	2	2	2	2	2	2	12
4 wt%	2	2	2	2	2	2	12
		Total specimens					48

Table 4.5 Distribution of above GFRP nanocomposite specimen for accelerated degradation in 45°C NaOH Solution (5% by weight of water)

Specimen Name	No. of specimens						Total specimens
	Normally Cured		Cured at 100^0C		Postcured		
	Tensile	Bending	Tensile	Bending	Tensile	Bending	
0.5 wt%	2	2	2	2	2	2	12
2 wt%	2	2	2	2	2	2	12
3 wt%	2	2	2	2	2	2	12
4 wt%	2	2	2	2	2	2	12
		Total specimens					48

5.1 PHYSICAL CHARACTERISTICS

5.1.1 X-ray diffraction test

The X-ray diffraction was conducted on the samples containing different concentration of nanoclay. X-ray diffractometer gives the values of d-spacing and 2θ for different samples of epoxy nanoclay nanocomposites.. The diffraction peak of Closite 30B comes out at an angle 2θ = 4.8 and corresponding d-spacing value with the help of bragg's law is d = 18.2, Fig 5.1 shows the X-Ray diffractrogram of epoxy/clay nanocomposites (a) 0.5 wt% nanoclay (b) 2 wt% nanoclay (c) 3 wt% nanoclay , (d) 4 wt% nanoclay.

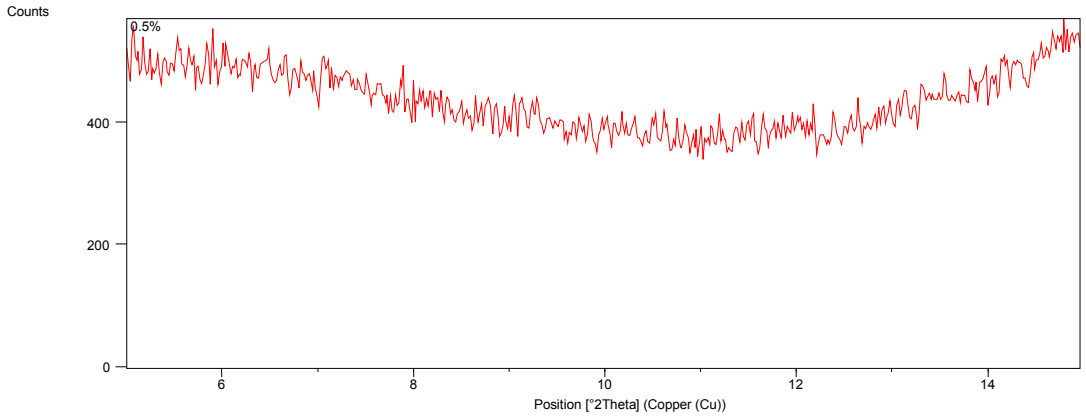

(a)

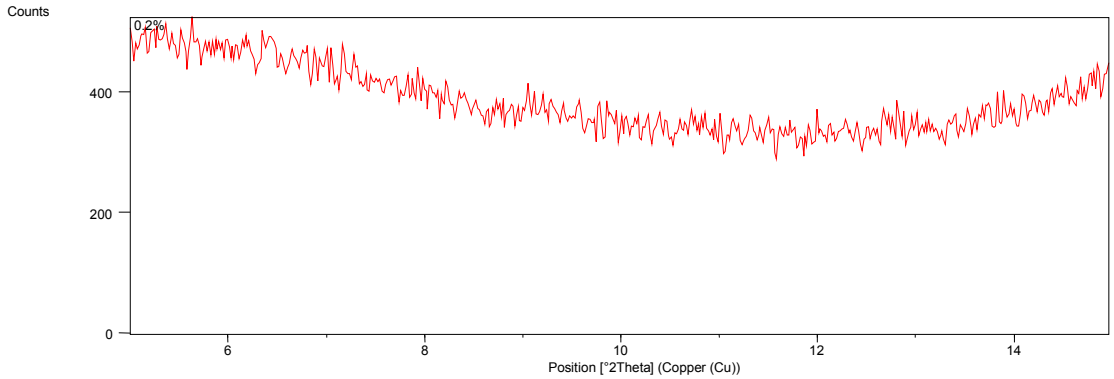

(b)

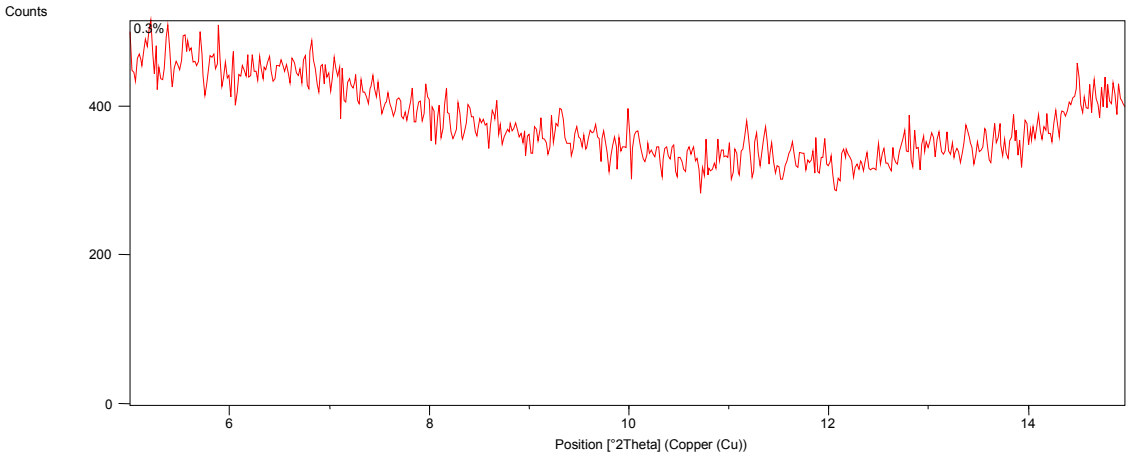

(c)

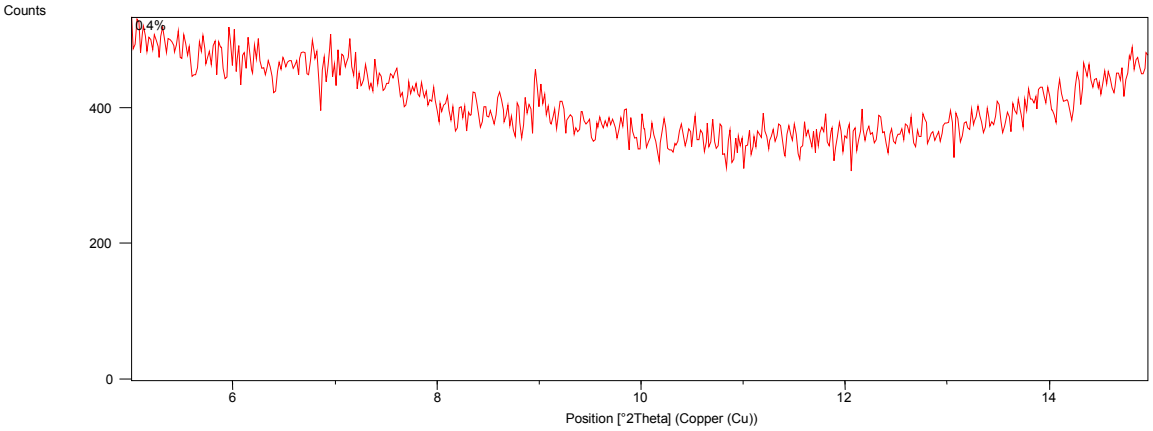

(d)

Fig 5.1 X-Ray diffractrograms of epoxy/clay nanocomposites

The absence of peaks in diffraction pattern indicates formation of exfoliated nanocomposites at all levels of nanoclay loading.

5.2 MECHANICAL PROPERTIES

5.2.1 Microhardness

5.2.1.1 Specimen for Microhardness

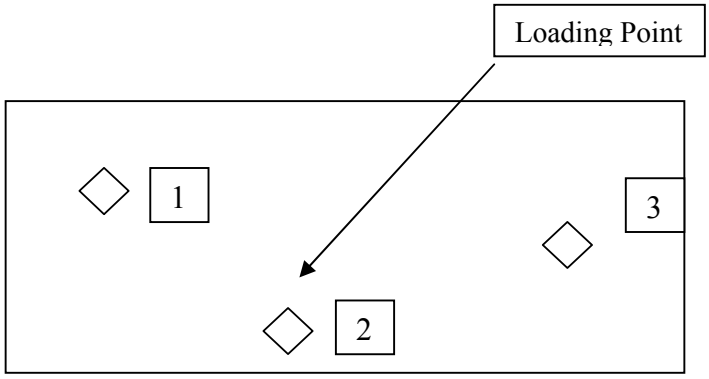

Fig. 5.2 Location of indents in specimen

The micro-hardness of epoxy & nanoclay specimen manufactured at different nanoclay loading was measured. The table 5.1 shows the experimental observations of the nanocomposites with different nanoclay contents. An average hardness was calculated by taking measurements at 3 points in each specimen Fig 5.3 shows the results of vicker hardness plotted against nanoclay loading.

Table 5.1 Micro hardness values for diff. nanoclay loading of normally cured sample

Nanoclay Loading / Loading Points	Micro hardness values			
	0.5 wt%	**2 wt%**	**3 wt%**	**4 wt%**
Point 1	6.957	7.281	5.621	5.504

Point 2	6.079	8.167	4.435	6.235
Point 3	6.079	7.157	5.789	6.032
Average	**6.372**	**7.535**	**5.282**	**5.927**

The maximum hardness has been measured in specimen having 2wt% nanoclay content. A decrease in values of hardness was observed on further increasing the nanoclay content; the hardness decreases in a drastic manner from 7.535 Hv (2 wt% of nanoclay) to 5.282 Hv (3 wt% of nanoclay). This is consistent with research carried out by other researches

Table 5.2 Microhardness values for diff. nanoclay loading samples of postcured sample

Nanoclay Loading → / Loading Points ↓	**Micro hardness values**			
	0.5 wt%	**2 wt%**	**3 wt%**	**4 wt%**
Point 1	6.7038	8.3566	5.3463	6.4427
Point 2	6.9546	8.0912	5.5172	6.7407
Point 3	6.7416	8.7601	5.6978	5.9847
Average	**6.8**	**8.405**	**5.8**	**6.385**

Thus adding a small amount of nanoclays into polymer-based materials could potentially enhance hardness of the material with the nanoclay content. However, it is also reasonable to believe that it should have an optimal limit depending on choice of constituent material and processing conditions. It was suspected that the nanoclays might retard the chemical reaction, and so cause incomplete curing process of the composites. For all samples with high nanoclay content, the matrix might not be fully cured.

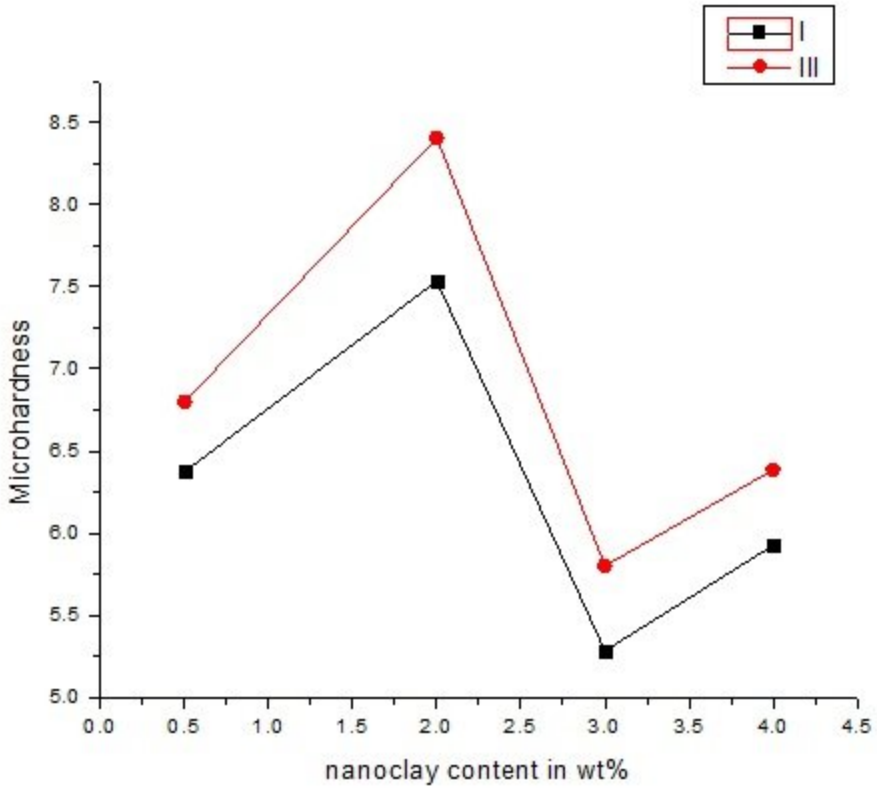

Fig 5.3 Graph showing the effect of postcuring

Fig 5.3 shows that with postcuring hardness increases for all specimen in comparison to the specimen cured under ambient conditions and the highest value of hardness was seen in specimen containing 2wt% at nanoclay and cured under conditions III as the highest value of microhardness for specimen I = 7.535 but for specimen III the highest value of microhardness = 8.4027.

5.2.2 TENSILE AND THREE-POINT BENDING TESTS

Fig 5.4 shows the tensile strength comparison between material I, II & III and Fig 5.5 shows the flexural strength comparison between material I, II & III.

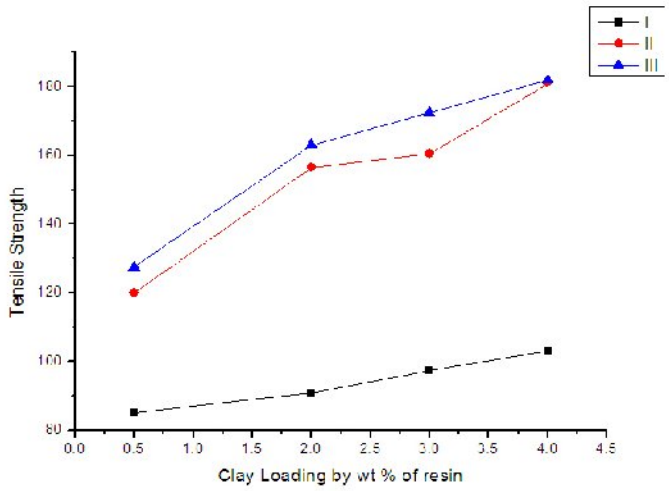

Fig 5.4 Tensile strength comparison in material I, II& III

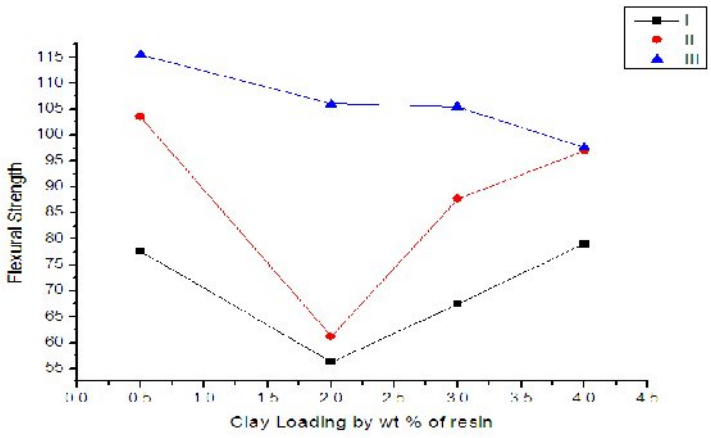

Fig 5.5 Flexural strength comparison in material I, II& III

These graphs (in fig 5.4, 5.5) depict that there is large and relative increase in the tensile strength of the material prepared under conditions II & III than the material prepared under condition I as the tensile strength of the material after postcuring increased to 179MPa from 85MPa (for 4wt% nanoclay) as shown in figure above . The increase in strength of the material must be due to the introduction of the nanoclay, which hindered the molecular movement of polymer chains.

5.2.2.1 Tensile testing results of the samples simple and hygrothermally loaded

Abbreviations used in Tables I = Normally cured sample

II = Sample cured at100^0C.

III = Postcured sample

Table 5.3 Degradation of nanocomposites in water tank at 45^0C

Water Tank at 45^0C											
No. of Days	**Sample Name**	**Sample No.**	**Tensile Modulus(MPa)**			**Tensile Strength(MPa)**			**Strain At Tensile Strength %**		
			I	II	III	I	II	III	I	II	III
0 Day	**0.5wt %**	**1**	474	2410	1300	97.8	121	125	2.21	1.81	2.40
		2	964	1870	966	72.7	119	130	1.77	2.03	2.15
	2wt%	**1**	535	1120	1300	109	163	162	2.24	1.84	1.98
		2	838	679	1310	72.7	150	164	1.97	2.06	2.06
	3wt%	**1**	1730	2720	1910	90	175	174	1.72	1.90	2.08
		2	1810	974	1350	105	146	171	2.28	2.31	1.86
	4wt%	**1**	1500	1130	1670	106	182	182	1.76	2.18	1.98
		2	520	1790	2150	100	180	182	1.98	2.04	1.76
30 Days	**0.5wt %**	**1**	1460	295	678	86.7	99	110	1.67	2.11	2.58
		2	500	295	2150	86.7	102	111	2.03	2.11	1.95
	2wt%	**1**	248	577	590	89.9	167	130	2.84	3.11	3.15
		2	1950	387	590	89.9	91.3	125	1.98	2.04	3.15
	3wt%	**1**	2090	709	1493	100	166	160	1.63	2.66	2.31
		2	6790	911	1480	91.8	145	161	1.12	1.47	2.08
	4wt%	**1**	950	1710	2590	102	182	170	1.97	2.01	2.61
		2	2600	2160	1110	98	157	173	1.38	1.86	2.55

Table 5.4 Degradation of nanocomposites in NaOH tank at 45^0C

NaOH at 45^0C											
No. of Days	**Sample Name**	**Sample No.**	**Tensile Modulus**			**Tensile Strength(MPa)**			**Strain at Tensile Strength %**		
			I	**II**	**III**	**I**	**II**	**III**	**I**	**II**	**III**
0 Day	**0.5wt%**	**1**	474	2410	1300	109	163	144	2.21	1.81	2.40
		2	964	1870	966	72.7	182	97.6	1.77	2.03	2.15
	2wt%	**1**	535	1120	1300	97.8	121	162	2.24	1.84	1.98
		2	838	679	1310	72.7	119	169	1.97	2.06	2.06
	3wt%	**1**	1730	2720	1910	109	175	174	1.72	1.90	2.08
		2	1810	974	1350	105	146	138	2.28	2.31	1.86
	4wt%	**1**	1500	1130	1670	106	182	182	1.76	2.18	1.98
		2	520	1790	2150	86.2	180	176	1.98	2.04	1.76
30 Days	**0.5wt%**	**1**	418	899	227	4.07	35.2	23.1	0.499	0.907	.775
		2	1030	685	871	11.1	31.4	11.2	0.490	1.35	1.06
	2wt%	**1**	473	485	728	7.31	2.53	22.8	0.858	0.511	0.670
		2	509	620	920	7.48	4.11	6.44	0.575	0.364	0.402
	3wt%	**1**	1370	1310	1680	11.7	16.6	14.12	0.472	0.910	0.716
		2	957	882	789	7.75	16.4	16.7	0.506	0.554	0.623
	4wt%	**1**	663	1060	1040	9.61	13.3	12.4	0.730	0.708	0.785
		2	643	880	958	11.9	10.8	20.7	0.521	0.899	0.775

5.2.2.2 Degradation in tensile strength of nanocomposites in water tank at 45^0C in fig 5.6 (a) 0.5wt% nanoclay (b) 2wt% nanoclay (c) 3wt% nanoclay (d) 4wt% nanoclay

Fig 5.6 shows the degradation in tensile strength of the nanocomposites in water tank at 45^0C for different clay contents in them

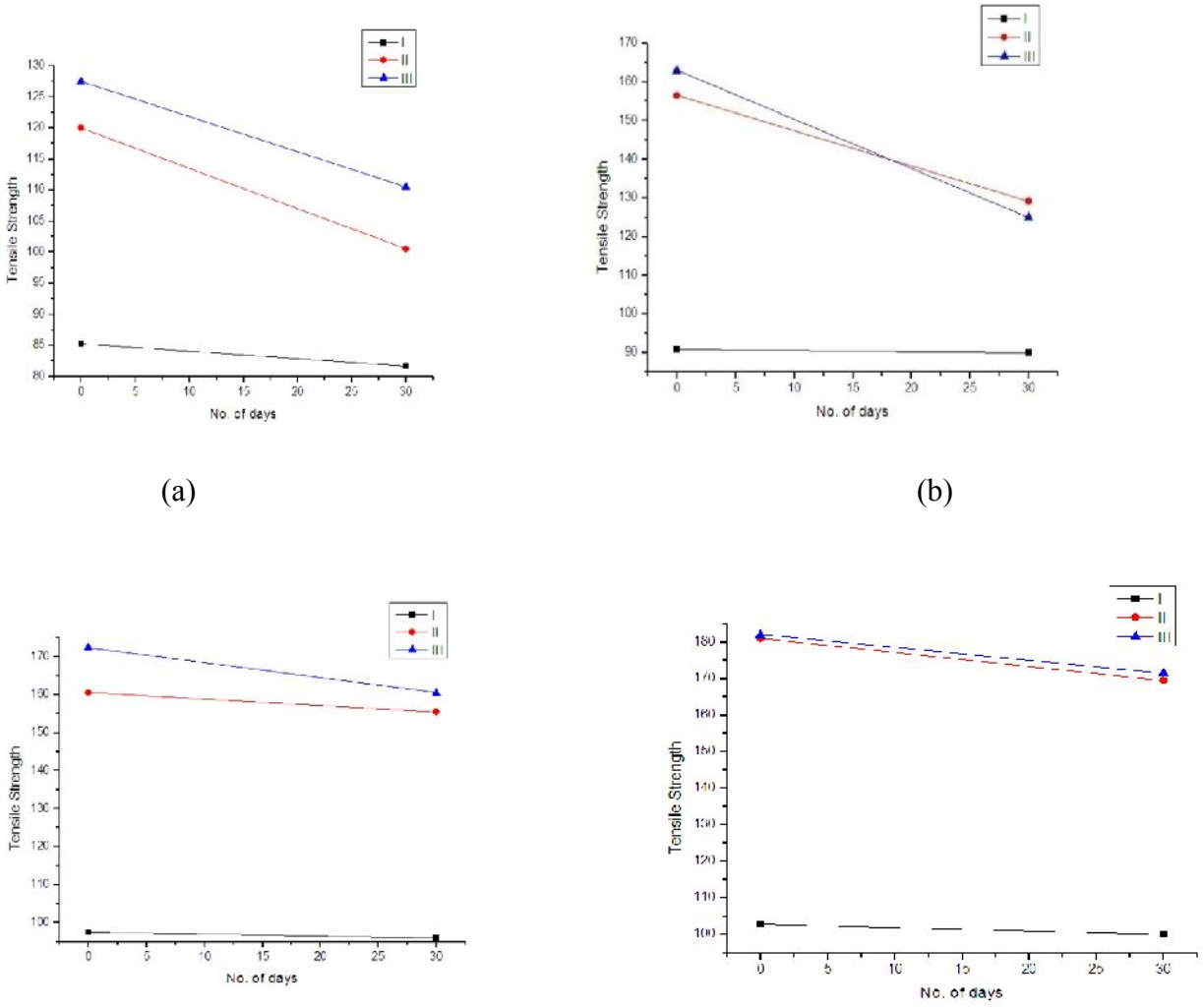

(a) (b)

(c) (d)

Fig 5.6 Degradation in tensile strength of nanocomposites in water

5.2.2.3 Degradation in tensile strength of nanocomposites in NaOH tank at 45^0C in fig 5.7 (a) 0.5wt% nanoclay (b) 2wt% nanoclay (c) 3wt% nanoclay (d) 4wt% nanoclay

Fig 5.7 shows the degradation in tensile strength of nanocomposites in NaOH tank at 45^0 C for different clay contents in them.

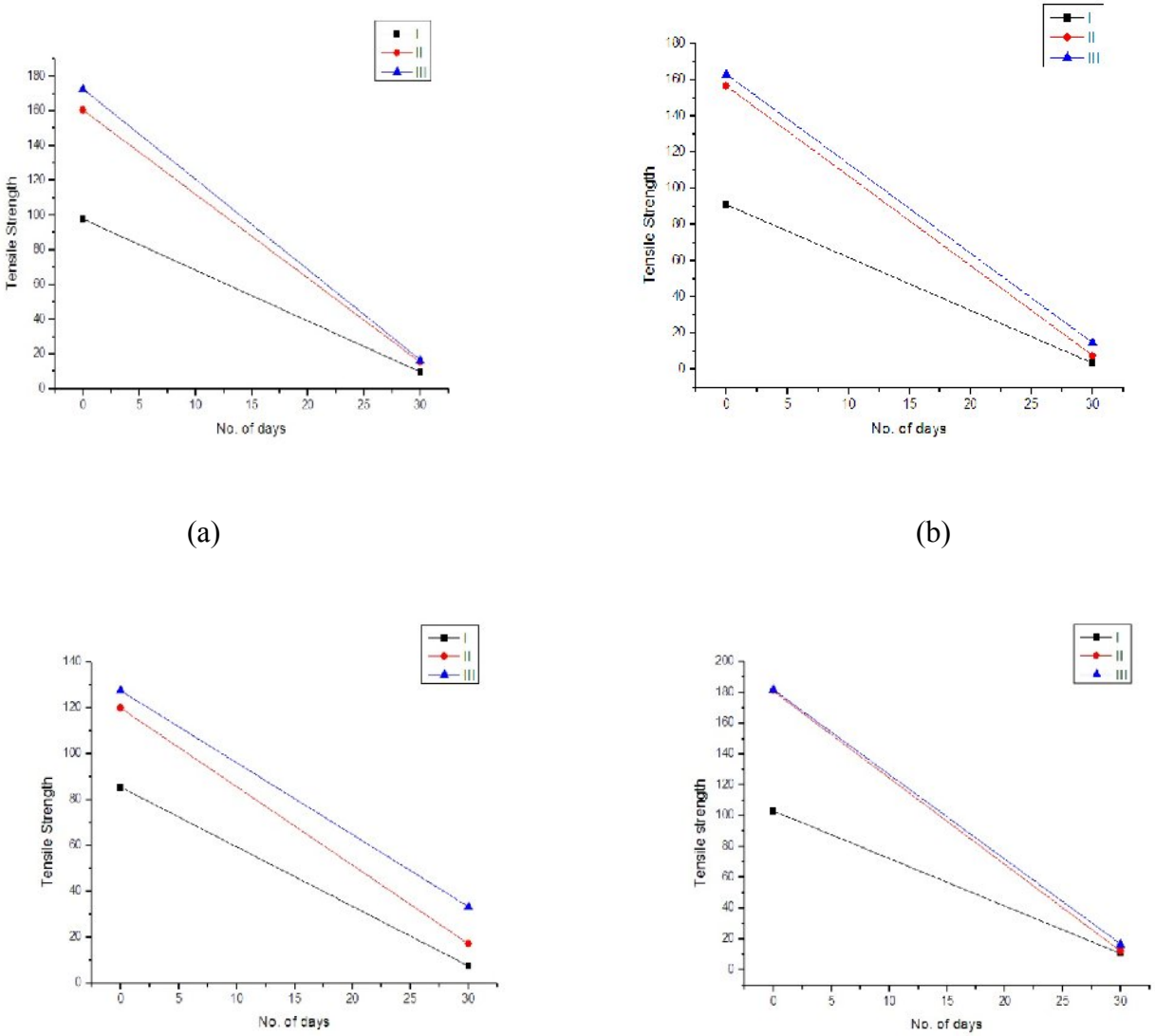

Fig 5.7 Degradation in tensile strength of nanocomposites in NaOH

These graphs (fig 5.6 and fig 5.7) of tensile strength depict that there is not much difference between the strength of the material cured under condition II & material cured under condition

III but there is significant increase in the strength of the material which has been cured at 100^0C than the material which is cured at ambient temperature . For example a sample(4 wt% nanoclay) when cured at ambient temperature had strength 103MPa and after postcuring its strength increased to 179MPa.

5.2.2.4 Three-point bending test results of nanocomposites under hygrothermal loading

Table 5.5 Results of samples for water bath at 45^0C

Water Tank at 45^0C											
No. of Days	**Sample Name**	**Sample No.**	**Elastic Modulus**			**Flexural Strength(MPa)**			**Deformation At Max. Force %**		
			I	II	III	I	II	III	I	II	III
0 Day	**0.5wt %**	1	5.96	5.72	6.30	105	84.6	94.0	1.6	1.6	1.7
		2	9.25	3.73	6.07	126	70.6	113	1.9	1.9	2.3
	2wt%	**1**	4.43	5.29	5.36	102	72	65.8	1.9	2.2	1.4
		2	4.99	1.84	4.41	110	50.2	46.6	1.8	1.6	1.1
	3wt%	**1**	7.02	5.10	4.26	114	93.1	72.2	1.6	1.3	2.3
		2	6.52	6.07	3.04	97.7	82.3	62.7	1.2	1.2	1.7
	4wt%	**1**	3.90	4.08	4.16	72.6	104	101	2.8	1.7	1.8
		2	4.63	5.97	7.22	85.4	89.8	94.2	2.1	2.2	1.5
30 Days	**0.5wt %**	**1**	1.43	1.40	1.39	42.5	37.4	63.5	2.4	2.4	3.9
		2	1.53	1.39	1.31	51.6	40.3	54.9	3.1	2.4	3.0
	2wt%	**1**	1.32	1.27	1.13	44.5	30.7	29.9	3.6	2.0	2.1
		2	1.33	1.50	1.14	46.3	25.2	25.5	3.4	1.9	2.3
	3wt%	**1**	1.43	1.27	.802	50.0	30.5	30.6	2.3	1.7	2.3
		2	1.36	1.27	.809	39.5	54.7	42.5	2.5	2.8	3.4
	4wt%	**1**	1.40	1.13	1.05	33.0	42.3	64.8	2.7	3.3	3.7
		2	1.34	1.19	1.13	34.3	48.3	65	3.0	3.5	3.7

Table 5.6 Results of samples from NaOH bath at 45^0C

NaOH at 45^0C											
No. of Days	**Sample Name**	**Sample No.**	**Elastic Modulus**			**Flexural Strength(MPa**			**Deformation At Max. Force %**		
			I	II	III	I	II	III	I	II	III
0 Day	**0.5wt %**	**1**	5.96	5.72	6.30	105	84.6	94.0	1.6	1.6	1.7
		2	9.25	3.73	6.07	126	70.6	113	1.9	1.9	2.3
	2wt%	**1**	4.43	5.29	5.36	102	72	65.8	1.9	2.2	1.4
		2	4.99	1.84	4.41	110	50.2	46.6	1.8	1.6	1.1
	3wt%	**1**	7.02	5.10	4.26	114	93.1	72.2	1.6	1.3	2.3
		2	6.52	6.07	3.04	97.7	82.3	62.7	1.2	1.2	1.7
	4wt%	**1**	3.90	4.08	4.16	72.6	104	101	2.8	1.7	1.8
		2	4.63	5.97	7.22	85.4	89.8	94.2	2.1	2.2	1.5
30 Days	**0.5wt %**	**1**	1.38	1.64	1.33	19.0	43.6	25.5	0.99	1.8	1.3
		2	1.46	1.70	1.38	19.9	32.4	26.5	1.0	1.4	1.3
	2wt%	**1**	1.56	1.47	1.44	27.7	18.9	18.9	1.3	0.93	0.93
		2	1.58	1.44	1.47	20.6	24.0	24.0	0.93	1.6	1.6
	3wt%	**1**	1.40	1.23	1.40	19.1	20.0	25.8	0.98	1.2	1.3
		2	1.78	1.38	1.85	24.3	34.2	46.6	0.95	1.5	1.7
	4wt%	**1**	0.852	1.72	1.90	14.5	18.3	27.3	1.1	1.1	1.0
		2	1.50	1.36	1.76	24.7	18.0	23.9	1.1	0.93	0.96

5.2.2.5 Degradation in flexural strength of nanocomposites in water tank at 45^0C in fig 5.8 (a) 0.5wt% nanoclay (b) 2wt% nanoclay (c) 3wt% nanoclay (d) 4wt% nanoclay

Fig 5.8 shows the degradation in flexural strength of nanocomposites in Water tank at 45^0 C for different clay contents in them.

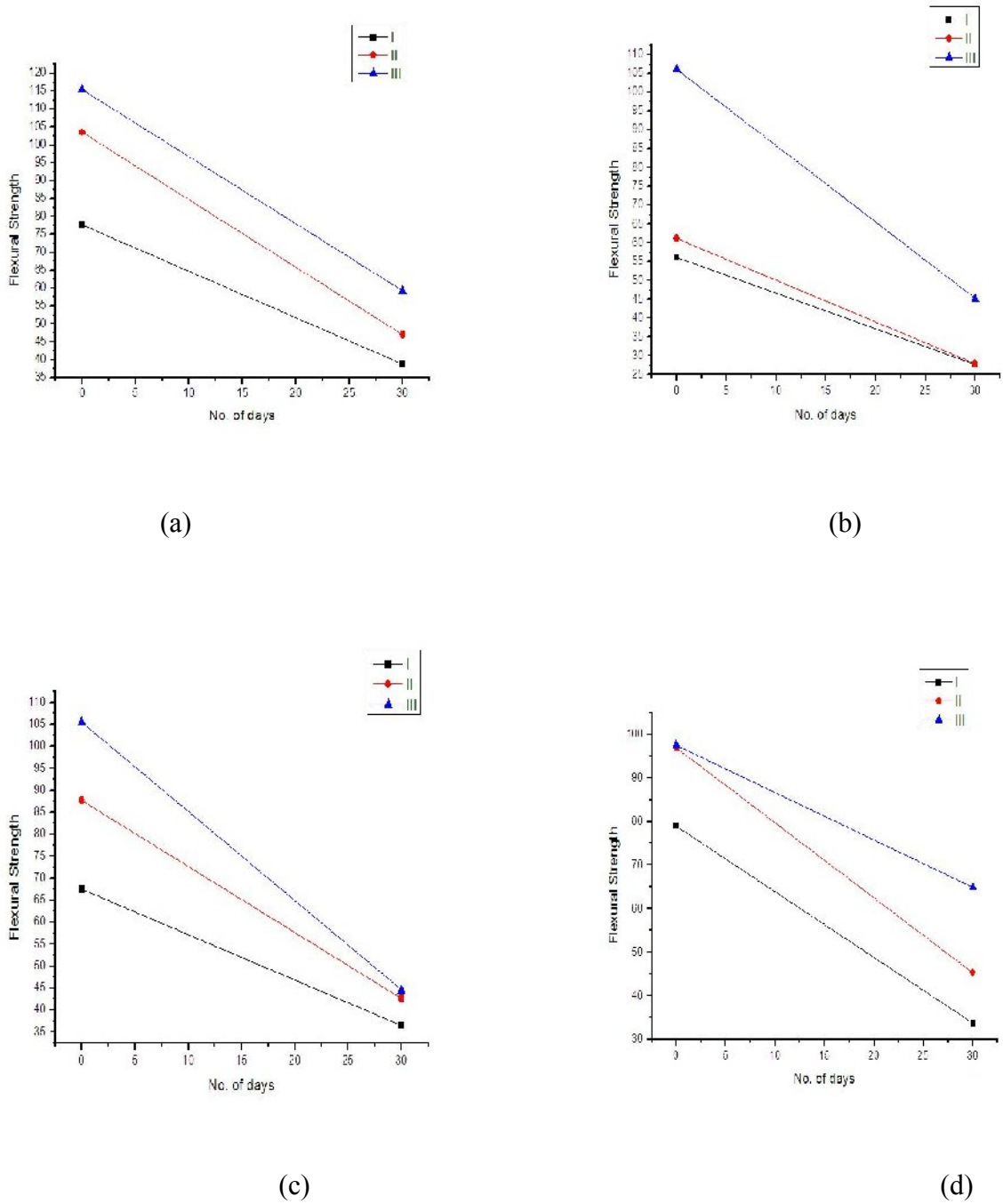

Fig 5.8 Degradation in flexural strength of nanocomposites in water tank

Fig 5.2.2.6 Degradation in flexural strength of nanocomposites in NaOH tank at 45^0C in fig 5.9 (a) 0.5wt% nanoclay (b) 2wt% nanoclay (c) 3wt% nanoclay (d) 4wt% nanoclay

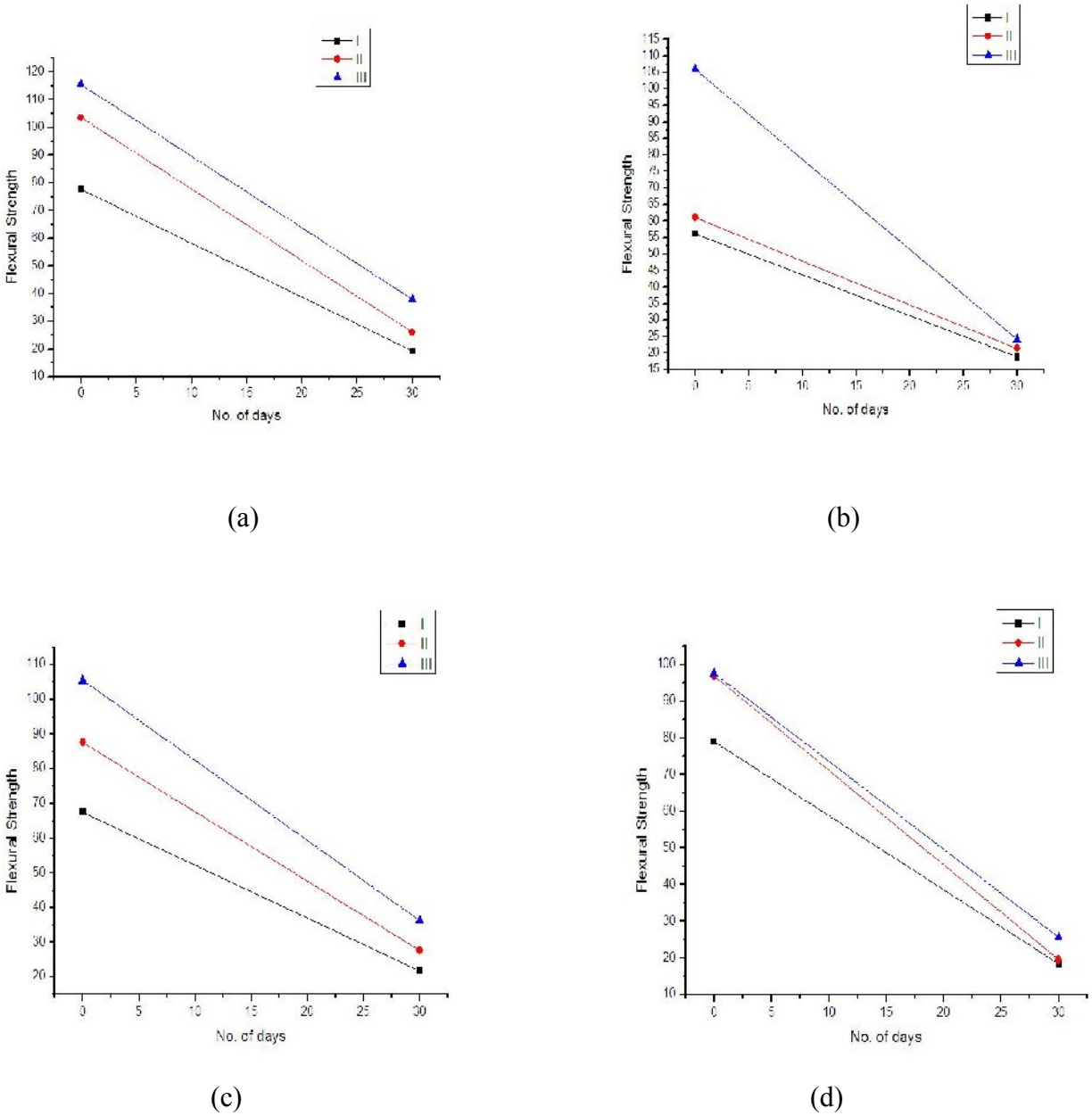

Fig 5.9 Degradation in flexural strength of nanocomposites in NaOH tank

These graphs(fig 5.8 and 5.9) show that there is a significant increase in the flexural strength as the effect of post curing, may be due to more efficient crosslinking of polymer. There is constant decrease in flexural strength after degradation in water but when degraded in NaOH the decrease in flexural strength in more i.e. degradation in NaOH is more as compared to water. Increase in

the flexural strength is more between the material cured under condition II & material cured under condition I except for the specimen with 2wt% nanoclay But there is not any prominent increase seen in the graphs of flexural strengths of material cured under condition II and III

5.2.2.7 Tensile strength of material I, II& III after degradation in (a) water (b)NaOH

Fig 5.10 shows the tensile strength of material after degradation in water and NaOH

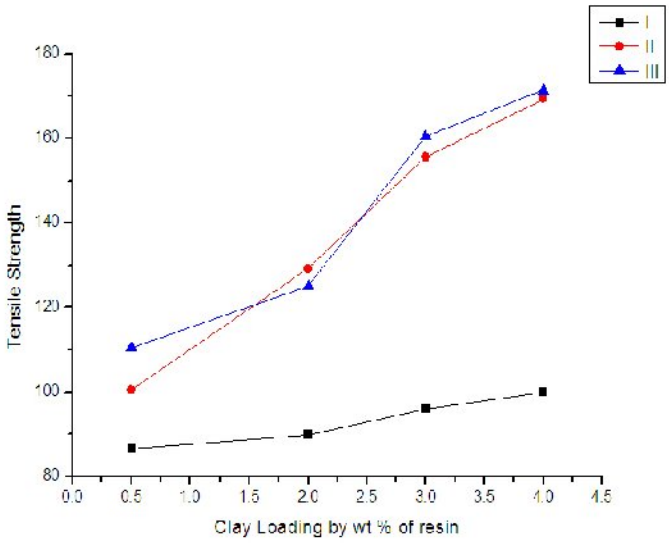

Fig 5.10 (a)

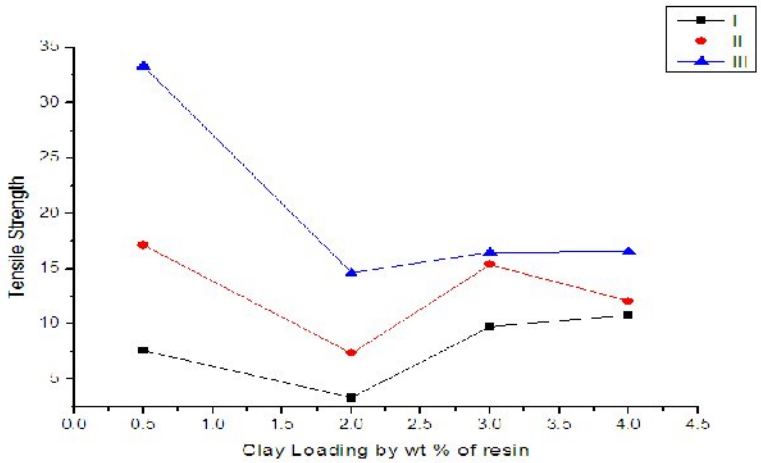

Fig 5.10 (b)

5.2.2.8 Flexural strength of material I, II& III after degradation in (a) water (b)NaOH

Fig 5.11 shows the tensile strength of material after degradation in water and NaOH

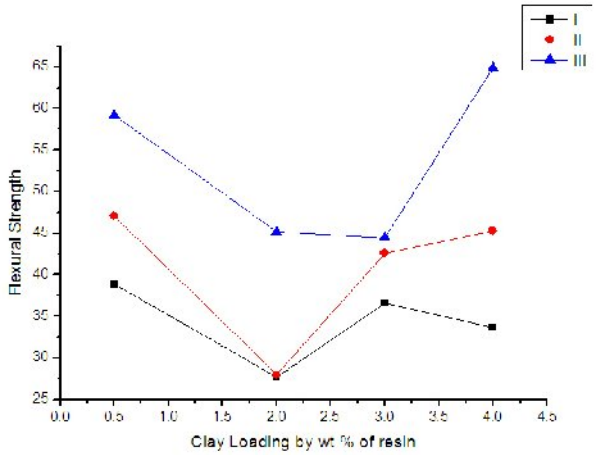

Fig 5.11(a)

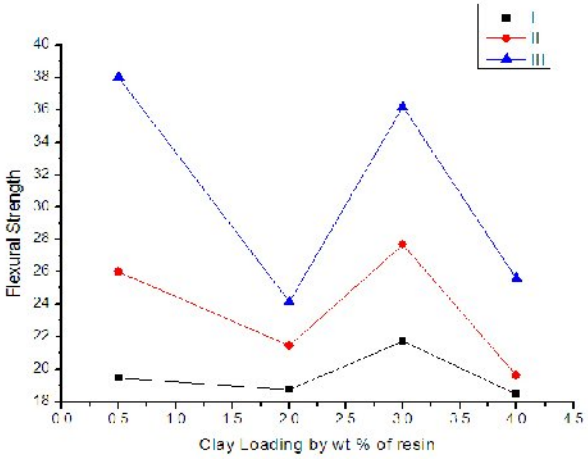

Fig 5.11(b)

Fig 5.10 (a) and fig 5.11(a) shows the effect of water immersion on tensile and flexural strengths of the specimen. A decrease in strength of all specimen is observed. This may be attributed to capability of the water molecules to penetrate through the epoxy network. Mechanical properties were found to degrade with time with both water and alkaline medium but the degradation was prominent in the case of degradation in alkaline medium. It was observed from the graphs that as the clay content in the specimen increases the rate of degradation in alkaline medium also increases.

6.1 Conclusion

Fiber reinforced nanocomposites have been manufactured using glass fiber as reinforcement and an epoxy mixed with closite 30B® as matrix and then were examined before and after hygrothermal loading. Exfoliation of nanoclay in epoxy was observed in samples from XRD results. Microhardness, tensile and three point bending tests were performed on the specimen prepared as per the standards. It was found that the microhardness of the nanocomposites increased with postcuring. Tensile strength and flexural strength of the postcured sample (III) was highest of all of the three specimens followed by the sample cured at 100^0C (II) and lowest for the sample cured at ambient temperature (I). This is probably due to better exfoliation of clay platelets at higher temperature during curing. This effect of better exfoliation & higher mechanical properties on application of thermal energy has also been reported for different polymer system. There was an increase in the value of strength with increase in clay content in the specimen. Durability studies were conducted on nanocomposites by exposing to water and alkaline medium for a period of one month and evaluating the mechanical property affected by degradations. Mechanical properties were found to degrade with time with both water and alkaline medium but the degradation was more prominent in the case of degradation in alkaline medium . There was maximum degradation seen in postcured sample which has been degraded in NaOH solution. It was observed from the graphs that as the clay content in the specimen increases the rate of degradation in alkaline medium also increases.

6.2 Future scope

1. The experiment can be done by placing the fiber sheets at different orientations other than $[0^0,90^0,0^0]$.
2. Mode of heating can be varied for example by microwave heating.
3. Duration of heating can be varied.
4. The strength of alkaline aqueous solution can be varied to study the rate of degradation.
5. Experiments can be repeated with other nanofillers.

REFERENCES

1. **Alexandre M,** (2000), Polymer-layered Silicate Nanocomposites: Preparation, Properties and uses of a New Class of Materials, Mater. Sci. Eng. Rep., 28, 1-63.
2. **Avila A, Almir S and Marcelo I.,** (2006), A study on nanostructured plates behaviour under low-velocity impact loading. Material and design, 34, 28-41.
3. **Avila A, Horacio V. and Marcelo I.,** (2005), The nanoclay influence on impact response of laminated plates, Latin American journal of solids and structures, 3, 3-20.
4. **Berketis K, Tzetzis D and Hogg P.J,** (2007), The influence of long term water immersion ageing on impact damage behaviour and residual compression strength of glass fiber reinforced polymer (GFRP), Material and design, 29, 1300-1310.
5. **Biron, M.,** (1973), Thermosets and Composites-Technical Information for Plastics Users, New York: Elsevier.
6. **Chow W, Bakar A and Ishak Mohamad A.,** (2005), Water absorption and hygrothermal aging study on organomontomorrillonite reinforced polyamide6/polypropylene nanocomposites, Journal of applied polymer science, vol 98, 780-790.
7. **Edward M. Petrie,** (2004), Room Temperature or elevated temperature cure.
8. **F.H.Chowdhary, M.V. Hosur , S. Jeelani,**(2006), Studies on flexural and thermomechanical properties of woven carbon/nanoclay epoxy laminates,421,298-306.
9. **Gao Shang-Lin, Mader E and Plonka R.,** (2007), Nanocomposite coating for healing surface defects of glass fiber and improving interfacial adhesion, Composite science and technology, 68, 2892-2901.
10. **Hossain M. K., Imran K. A., Hosur M. V. and Jeelani S.,** (2011), Degradation of Mechanical properties of convectional and nanophased Carbon/Epoxy composites in seawater.
11. **Jena P,** (1996), Nanostructured materials**,** Nova Science New York.
12. **Kornmann X, Rees M, Thomsan Y, Necola A, Barbezat M and Thomsan R,** (2005), Epoxy layered silicate nanocomposite as matrix in glass fiber-reinforced composites, Composite science and technology, 65, 2259-2268.

13. **Lei Wang, Ke Wang, Ling Chen and Chaobin He,** (2006), Hydrothermal Effects on the Thermo-mechanical Properties of High Performance Epoxy/Nanoclay Nanocomposites, Polymer engineering science, 46, 215–221.
14. **Lin Li-Yu, Lee Joong-Hee, Hong Chang-Eui, Yoo Gye-Hyoung, Advani Suresh G,** (2005), Preparation and characterization of layered silicate/glass fiber/epoxy hybrid nanocomposites via vacuum-assisted resin transfer moulding (VARTM), Composites Science and Technology 66 (2006) 2116–2125.
15. **Manjunatha C.M, Taylor A.C, Kinloch A.J and Sprenger S,** (2009), The tensile fatigue behavior of a silica nanoparticle-modified glass fiber reinforced epoxy composites, Composite science and technology, 70, 193-199.
16. **Njuguna J and Pielichowski K,** (2003),Advanced Engineering Materials, 5, 769.
17. **Quaresimin M. and Varley R. J,** (2007). Understanding the effect of nano-modifier addition upon the properties of fiber reinforced laminates, Composite science and technology, 68, 718-726.
18. **Rumiana K,** (1994), Thermoset Nanocomposites for Engineering Applications.
19. **Sakaki H and Noge H., eds,** (1994), Springer Verlag, Berlin.
20. **Sinha R. S., Okamoto M.,** (2003), Polymer/layered silicate nanocomposites: a review from preparation to processing, Prog. Polym. Sci., 28, 1539–1641.
21. **Wang H, Zeng C, Elkovitch M and Koelling W. K,** (2001), Processing and properties of polymeric nanocomposites, Polymer engineering and science, 41, 11.
22. **Wetzel B, Rosso P, Haupert F and Friedrich K,** (2006), Epoxy nanocomposite-fracture and toughening mechanisms, Engineering fracture mechanics, 73, 2375-2398.
23. **Yasmin A, Luo J.J, Abot J.L, Danial I.M,** (2006), Mechanical and thermal behavior of nanoclay/epoxy nanocomposites, Composite science and technology, 66, 2415-2422.
24. **Zafar A, Bertocco F, Schjodt-Thomsen J and Rauhe J.C**, (2012), Investigation of the long term effects of moisture on carbon fibre and epoxy matrix composites, Composite science and technology.
25. **Zainuddin S, Hosur M.V, Zhou Y, Kumar Ashok and Jeelani S,** (2010), Durability study of neat/nanophased GFRP composite subjected to different environmental conditioning, Material science and engineering, A 57, 3091-3099.